The Inject-Mix-React-Separate-and-Quantitate (IMReSQ) approach to studying reactions in capillaries

Svetlana M. Krylova, Victor Okhonin, Christopher J. Evenhuis, Sergey N. Krylov

A capillary or a narrow channel is an attractive medium for studying reactions. A capillary can serve as (i) a microreactor for carrying out a reaction in a nanoliter volume and (ii) a separation column to separate the reaction products prior to their quantitation. The term ''Inject-Mix-React-Separate-and-Quantitate'' (IMReSQ) includes all analyses of reactions in capillaries that involve these five steps. We analyze these steps in detail and formulate the requirements for them to be generic and quantitative.

Keywords: Capillary; Diffusion; Electrophoresis; IMReSQ; Injection; Kinetics; Microanalysis; Mixing; Reaction; Separation

Svetlana M. Krylova, Victor Okhonin, Christopher J. Evenhuis, Sergey N. Krylov*
Department of Chemistry, York University, Toronto, Ontario, Canada M3J 1P3

1. Introduction

Capillaries in combination with an electric field are used as tools for studying mechanisms of chemical reactions, in particular, reaction kinetics. Kinetic methods can be classified in a number of ways. For the purpose of this article, we split them into two broad categories: continuous and discontinuous methods. In continuous methods, reaction kinetics is recorded continuously as the reaction progresses. In discontinuous methods, the reaction is stopped at different times after the start and the reaction components are then quantitated; every experiment generates a single time point in the kinetics.

Continuous methods for kinetic studies in capillaries using an electric field fall in the realm of kinetic capillary electrophoresis (KCE), which is CE of species that interact during electrophoresis. A requirement for KCE is that at least some of the reacting species move with different velocities in the electric field.

An electric field in KCE serves two functions. First, it mixes or separates interacting species, thus, facilitating forward and backward processes of the reaction. Second, it moves the reacting species with different velocities and creates the space distribution of species that is directly linked to the time distribution of species. The time distribution of species concentrations is, *per se*, kinetics. The links between the space coordinate (x) and time coordinate (t) of the species are trivial, assuming that the velocity (v) is known: $x = vt$. Figuratively speaking, the second function of an electric field in KCE is to pull the paper in a chart recorder.

Discontinuous methods for kinetic studies in capillaries using an electric field fall either in the realm of classical CE or in the realm of the conceptual term ''Inject-Mix-React-Separate-and-Quantitate'' (IMReSQ, which spells out and emphasizes the importance of all essential steps in the analysis). In a classical CE approach, the reactants are mixed and reacted in a vial outside the capillary, the reaction is stopped, and then a small volume of the reaction mixture is injected into a capillary and the reaction components are separated and quantitated. This approach is trivial and does not deserve attention here. In an IMReSQ approach, a part of the capillary itself is used as a microreactor with two major goals: to decrease reagent consumption dramatically and to make the approach suitable for automation.

It is worthwhile to compare KCE and IMReSQ. In KCE, an electric field is applied during the reaction and the ''reaction'' and ''electric-field migration'' steps are merged. By contrast, in IMReSQ, it is not necessary to apply an electric field during

*Corresponding author.
Tel.: +1 416 736 2100x22345;
Fax: +1 416 736 5936.;
E-mail: skrylov@yorku.ca

0165-9936/$ - see front matter © 2009 Elsevier Ltd. All rights reserved. doi:10.1016/j.trac.2009.05.004

the course of the reaction. Moreover, in an ideal IMReSQ method, the reaction would proceed only during the ''reaction'' step and not during the ''injection'', ''mixing'', ''separation'' or ''quantitation'' steps. While both KCE and IMReSQ aim to study reactions in capillaries using an electric field, the two approaches are conceptually different and are not typically hybridized with the exception of using the ''Inject-Mix-and React'' (IMR) part of IMReSQ in KCE methods that require pre-equilibration before the analysis. The IMR-KCE combination would be useful for saving reactants and for automation [1].

KCE methods were reviewed recently [2] and are not a focus of this article. By contrast, IMReSQ as a general approach has not been reviewed and is the sole subject of this article.

When practical IMReSQ methods are developed, it is critical that correct performance criteria are taken into consideration. There are three essential performance criteria for the methods: they must be generic, quantitative and practical.

To be generic, IMReSQ methods have to be applicable to different chemical reactions and require minimal optimization of the five steps (injection, mixing, reaction, separation, and quantitation).

To be quantitative, IMReSQ methods have to produce an output result that can be used to find quantitative parameters (e.g., reaction-rate constants and stoichiometry coefficients). That can only be done if all steps are performed in a perfectly controlled way and if a mathematical approach is available to calculate concentrations of all reactants and products as functions of spatial coordinates and time.

To be practical, IMReSQ methods should be implementable with commercially available instrumentation. It is important to emphasize that, due to the sequential nature of processes in IMReSQ, the steps earlier in the sequence may influence the later steps in terms of the options available for technical implementation of the later steps. For the same reason, IMReSQ can be generic and quantitative only if every step in the sequence is generic and quantitative. Our analysis below confirms that IMReSQ is both generic and quantitative by considering these two performance criteria in individual steps of IMReSQ. To address the issue of practicality, we also discuss the instrumentation required and available for IMReSQ.

2. Injection

In-capillary mixing has several advantages over mixing of reactants in a container outside the capillary. Most importantly, in-capillary mixing avoids wastage of expensive reagents. Only nL of solutions are required for in-capillary mixing while μL are needed to mix reactants outside the capillary using conventional pipetters [3]. Moreover, pre-mixing of even a sub-set of reactants outside the capillary can lead to their degradation. The injection processes used to facilitate in-capillary mixing, namely pressure or electrokinetic injection, are familiar to all practitioners of CE so that there is no complexity added to that of operating conventional instrumentation.

To be generic, injection in IMReSQ should depend as little as possible on the nature of molecules so that the process of optimizing the injection is minimized. In addition, to be generic, an injection method has to facilitate separate injection of multiple reactants.

To facilitate quantitative analyses, injection has to be carried out in a perfectly controlled way so that the concentration profiles of reactants along the capillary length can be calculated. The only two practical ways of injection into the capillary are by electroosmosis or pressure (Fig. 1), which we consider separately.

2.1. Electroosmosis

An electroosmotic flow (EOF) occurs in fused-silica capillaries due to the deprotonation of silanol groups of silica, which, in essence, creates an immobile negative charge on the inner capillary wall and a mobile positive charge in the buffer next to the wall. If a voltage is applied to the ends of the capillary, these positive ions move along the electric field, dragging the buffer solution in the same direction, thus creating EOF [4].

EOF depends strongly on the chemistry of the inner capillary wall, the strength of the electric field, as well as the pH, composition and ionic strength of the buffer. The volume of the injected reactant plug can be easily adjusted by changing the strength of the electric field and the time of its application (Fig. 1A). While being quite a common way of injecting reactant into capillaries, EOF is not a generic means of injection. For example, EOF does not occur if the inner capillary walls are coated with a layer of non-ionizable material; such coatings are often used to suppress solute adsorption to the inner capillary walls [5]. The unique nature of EOF is the flat shape of its front, which does not depend on the velocity of EOF (Fig. 1A). The velocity of EOF can be measured experimentally, allowing the concentration profile of the injected reactant to be well defined. The length of the injected plug l is given by Equation (1):

$$l = \int_0^{t_{inj}} v(t)dt \quad (1)$$

where $v(t)$ is the velocity of EOF as function of time and t_{inj} is time of injection.

To be quantitative, the injection must be free of turbulence, as turbulence creates vortexes (i.e. stochastic hydrodynamic structures that cannot be predicted accurately). Turbulence does not appear when the velocity of injection is low. The theory of turbulence in

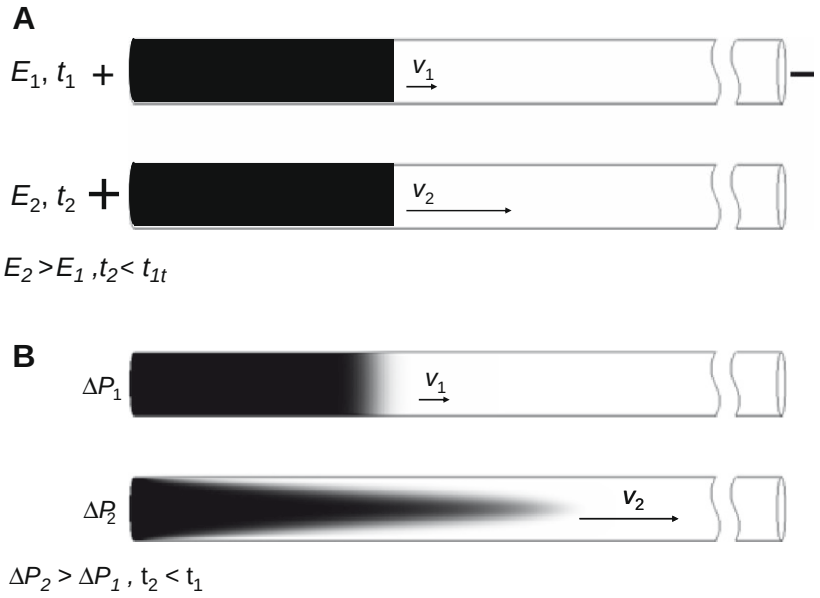

Figure 1. Representation of reactant injection into a capillary by: electroosmotic flow (**A**, artistic depiction) and differential pressure (**B**, computer simulation). The size of the injection plug in **A** is determined by the product of the electrical field strength (*E*) and the time for which it is applied (*t*) The font size used for + and − reflects the strength of *E*. In **B**, the size of the injection plug is determined by the pressure difference between the capillary inlet and the outlet (ΔP), and the time for which the pressure is applied. The computer simulation of panel **B** took into account two processes: pressure-driven flow and reactant diffusion in the transverse direction. The quantitative parameters in the simulation were chosen to illustrate that the front shape can range from rectangular to parabolic.

EOF has not yet been developed. We should appreciate that the standard criterion of instability for pressure-driven laminar flows, which requires that the Reynolds number (Re) be greater than 2000, is not applicable to EOF.

To conclude, EOF as a means of injection is quantitative for low velocities of injection, a condition that is easy to satisfy for narrow-bore capillaries. The mathematics describing EOF is very simple. However, EOF is not a generic means of injection, so its application in IMReSQ is limited.

2.2. Pressure

A reactant plug can be injected into a capillary by a pulse of differential pressure applied to the two ends of the capillary. Technically, there are two options: either pressure is applied to the injection end while the distal end remains open to the atmosphere or suction is applied to the opposite end while the injection end remains open to the atmosphere. The first approach allows creation of very high differential pressures, while the second approach is limited to a differential pressure of <1 atm.

To be quantitative, pressure-driven injection has to be non-turbulent. This requirement is similar to that for EOF-driven injection. If the velocity of injection is low enough (Re < 2000), which is readily achieved for narrow-bore capillaries, pressure-driven flow is laminar and controlled by two processes of mass transfer: hydrodynamic transfer and diffusion (both longitudinal and transverse). Both processes are non-stochastic, allowing the exact concentration profile of the injected plug to be calculated.

Equation (2), called Poiseuille's Equation, shows that the velocity (v) of a pressure-driven flow inside the capillary depends on the differential pressure (Δp), the fluid viscosity (η), the capillary length (L), the capillary inner radius (r_i), the distance from the center of the capillary (r), and the time (t):

$$v(r,t) = \frac{(r_i^2 - r^2)\Delta p(t)}{4\eta L} \quad (2)$$

At the center of the capillary ($r = 0$), Equation (3) shows that the velocity, $v_0(t)$, is a maximum:

$$v_0(t) = \frac{r_i^2 \Delta p(t)}{4\eta L} \quad (3)$$

but the velocity is zero at the inner walls of the capillary ($r = r_i$).

If transverse diffusion is negligible, the profile of the flow is parabolic (Fig. 2) and the length of the injection, $l(r)$, can be calculated using Equation (4):

$$l(r) = \int_0^{t_{inj}} v(r,t)dt = \int_0^{t_{inj}} \frac{(r_i^2 - r^2)\Delta p(t)}{4\eta L} dt \quad (4)$$

Diffusion can be neglected if the differential pressure is high enough to inject the required volume of the

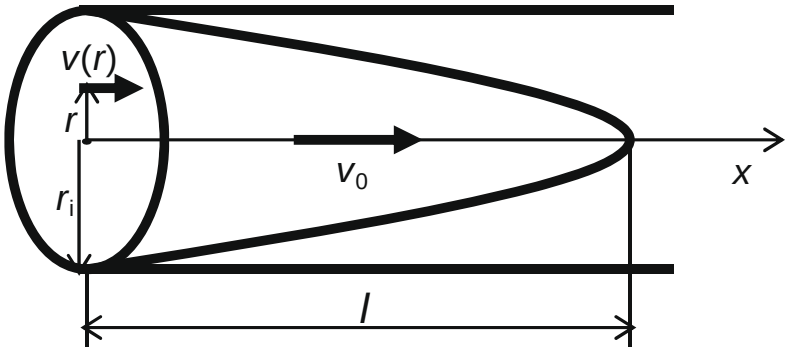

Figure 2. Major parameters used in the theoretical consideration of pressure-driven injection. r is the radial distance from the center of the capillary, r_i is its internal radius, $v(r)$ describes the velocity profile of the injection plug, v_0 is the velocity along the central axis, l is the length of the injection plug, and x is the distance from the inlet of the capillary in the longitudinal direction.

solution during a time interval that is considerably shorter than the characteristic time for transverse diffusion to occur.

By contrast, if transverse diffusion is very fast, the shape of the parabolic front is completely destroyed, leaving it flat, similar to that in Fig. 1A. In this case, Equation (4) simplifies to Equation (5):

$$l = \int_0^{t_{\text{inj}}} v_0(t)dt = \int_0^{t_{\text{inj}}} \frac{r_i^2 \Delta p(t)}{8\eta L} dt \tag{5}$$

If diffusion cannot be assumed too slow or too fast, the calculation of the exact concentration profile should take both the pressure-driven hydrodynamic flow and diffusion into consideration. The mass transfer by both the hydrodynamic flow and diffusion is mathematically described by the equations below [Equation (6)]:

$$\begin{aligned} &\frac{\partial C}{\partial t} = -v(r,t)\frac{\partial C}{\partial x} + D\left(\frac{\partial^2 C}{\partial x^2} + \frac{1}{r}\frac{\partial}{\partial r} r \frac{\partial C}{\partial r}\right) \\ &v(r,t) = v_0(t)\left[1 - \left(\frac{r}{r_i}\right)^2\right] \\ &D\frac{\partial C}{\partial r}\bigg|_{r=r_i} = 0 \end{aligned} \tag{6}$$

where, C is the concentration of the solute; D is its diffusion coefficient; r, r_i, $v(t)$, $v_0(t)$, and t are defined as above in this section, and x is the distance from the capillary inlet in the longitudinal direction. While the analytical solution of Equation (6) is challenging, the numerical solution can be found easily [6]. A numerical simulation of injection involving the two processes (pressure-driven translational movement and diffusion) was used to prepare Fig. 1B.

To take diffusion of a reactant into consideration, its diffusion coefficient should be known. There are a number of simple approaches to calculating a diffusion coefficient, with the only input parameters being the size (or the molecular weight) of the reactant, solvent viscosity and temperature. A simple approximation for D is given by the Stokes-Einstein Equation [Equation (7) [7]]:

$$D = \frac{k_B T}{6\pi\eta r_h} = \frac{k_B T}{\eta}\sqrt[3]{\frac{dN_A}{162\pi^2 M}} \tag{7}$$

where $k_B = 1.381 \times 10^{-23}$ J/K is Boltzmann's constant, T is the absolute temperature and r_h is the hydrodynamic radius of the molecule (assumed to be spherical), d is the density of the reactant in kg/m, $N_A = 6.022 \times 10^{-23}$/mol is Avagadro's constant and M is the molar mass of the reactant in kDa. Most approaches to calculating diffusion coefficients give only approximate values. There are also relatively simple ways to determine diffusion coefficient experimentally, including a capillary-based procedure that can be realized with a commercial CE instrument [8].

Equation (6) can be simplified to make it easier to analyze and to use. To do so, we introduce a characteristic length of the injected plug, l_{char}, which is related to the injection time, t_{inj}, as $l_{\text{char}} = t_{\text{inj}} v_{\max}$, where $v_{\max}$ is the maximum value of $v_0(t)$ during the time interval of injection. If Δp = constant during injection and $\Delta p = 0$ before and after injection, then v_0 = constant and $v_{\max} = v_0$. If we assume that l_{char} is much greater than the diameter of the capillary, $l_{\text{char}}/r_i >> 1$, the time required for transverse diffusion, t_r, will be much shorter than the time required for longitudinal diffusion, t_x, as shown in Equation (8):

$$\begin{aligned} &t_r = r_i^2/D, \quad t_x = l_{\text{char}}^2/D \\ &t_x/t_r = l_{\text{char}}^2/r_i^2 >> 1 \end{aligned} \tag{8}$$

The assumption leading to Equation (8) suggests that longitudinal diffusion can be ignored. This assumption is equivalent to the assumption that $\partial^2 C/\partial x^2$, in the top equation of Equation (6), is negligible. Accordingly, the differential equation in Equation (6) can be simplified to obtain the system of equations [Equation (9)] introduced by Taylor in 1953 [9]:

Table 1. York numbers for different diffusion coefficients, D, of the injected solute and different capillary radii, r_i, but for an identical injection time of 4 s

D (cm^2/s)	r_i (μm)		
	10	**25**	**37.5**
10^{-4}	4×10^{2}	64	28
10^{-5}	40	6.4	2.8
10^{-6}	4	0.64	0.28
10^{-7}	0.4	6.4×10^{-2}	2.8×10^{-2}
10^{-8}	4×10^{-2}	6.4×10^{-3}	2.8×10^{-3}
10^{-9}	4×10^{-3}	6.4×10^{-4}	2.8×10^{-4}

$$\frac{\partial C}{\partial t} = -v(r,t)\frac{\partial C}{\partial x} + D\frac{1}{r}\frac{\partial}{\partial r}r\frac{\partial C}{\partial r}$$
$$v(r,t) = v_0(t)\left[1-\left(\frac{r}{r_0}\right)^2\right] \qquad (9)$$
$$D\left.\frac{\partial C}{\partial r}\right|_{r=r_0} = 0$$

For simpler analysis, Equation (9) can be transformed into a dimensionless form if the following dimensionless variables and parameters [Equation (10)] are introduced:

$$c = C/C_{\max} \quad \text{dimensionless concentration}$$
$$\tau = tv_{\max}/l_{\text{char}} = t/t_{\text{inj}} \quad \text{dimensionless time}$$
$$\rho = r/r_i \quad \text{dimensionless capillary radius}$$
$$\chi = x/l_{\text{char}} \quad \text{dimensionless distance from capillary inlet}$$
$$\omega(\tau) = v_0(t)/v_{\max} \quad \text{dimensionless velocity for } \rho = 0 \qquad (10)$$

where, $C_{\max}$ is the concentration of the reactant in the vial prior to injection (this concentration is maximal, as it will only decrease upon pressure-driven injection) and $v_{\max}$ is the same as defined above. IMReSQ may involve injecting multiple plugs of different lengths (typically by varying the injection time). If the plug lengths are different, l_{char} is defined to be the length of the shortest plug. If the new variables from Equation (10) are applied to Equation (6), it can be transformed into the dimensionless system of equations [Equation (11)]:

$$\frac{\partial c}{\partial \tau} = -w(\tau)(1-\rho^2)\frac{\partial c}{\partial \chi} + \text{Yo}\frac{1}{\rho}\frac{\partial}{\partial \rho}\rho\frac{\partial c}{\partial \rho}$$
$$\left.\frac{\partial c}{\partial \rho}\right|_{\rho=1} = 0 \qquad (11)$$

where the parameter Yo, named ''York number'' after York University in Toronto, is given by Equation (12):

$$\text{Yo} = Dl_{\text{char}}/(v_{\max}r_i^2) = Dt_{\text{inj}}/r_i^2 = t_{\text{inj}}/t_r \qquad (12)$$

Yo is a single parameter in the first dimensionless equation of Equation (11), found by dividing the injection time by the time taken for complete lateral diffusion, so, if injection procedures are characterized by (i) similar initial and boundary conditions, (ii) identical time dependencies of the pressure [or identical $\omega(t)$], and (iii) similar Yo values, the injection will be similar and will generate similar final distribution of the injected reactant along the capillary axis.

It is instructive to compare Yo values that correspond to a typical range of diffusion coefficients of the reactant and capillary radii (Table 1).

Yo is a dimensionless value that characterizes the extent of transverse diffusion during plug injection. Yo can serve as a parameter to compare the shapes of pressure-injected plugs quickly and qualitatively for different sets of experimental parameters. As a rule, the lower Yo, the closer the shape of the injected plug front is to the parabolic one.

We have shown that, in the absence of turbulence, pressure is a quantitative means of injection. Pressure is also a generic method of injection. It can be applied to all types of molecule. The velocity of pressure-driven flow inside the capillary depends on only differential pressure, fluid viscosity, capillary length, capillary inner radius, distance from the center of the capillary and time [Equation (2)]. While diffusion can affect the shape of the plug front, the volume of the injected solution does not depend on the diffusion coefficient of a solute. Pressure can be used for injecting solutions into coated capillaries. Moreover, pressure-driven injection can be used to inject solutions of redox-active solutes that can degrade if injection is carried out by an electric field. To conclude, pressure-driven injections are both quantitative and generic.

3. Mixing

To be generic, mixing has to be applicable to all kinds of molecules and all kinds of capillaries. To be quantitative, mixing has to be non-turbulent and perfectly controlled. If turbulent phenomena (which are difficult to create in a narrow-bore capillary) are excluded, then mixing is limited to two processes: differential electrophoresis and diffusion (see Fig. 3). In-capillary mixing can be carried out by applying an electrical field or using suitable pressure pulses. While the processes are straightforward

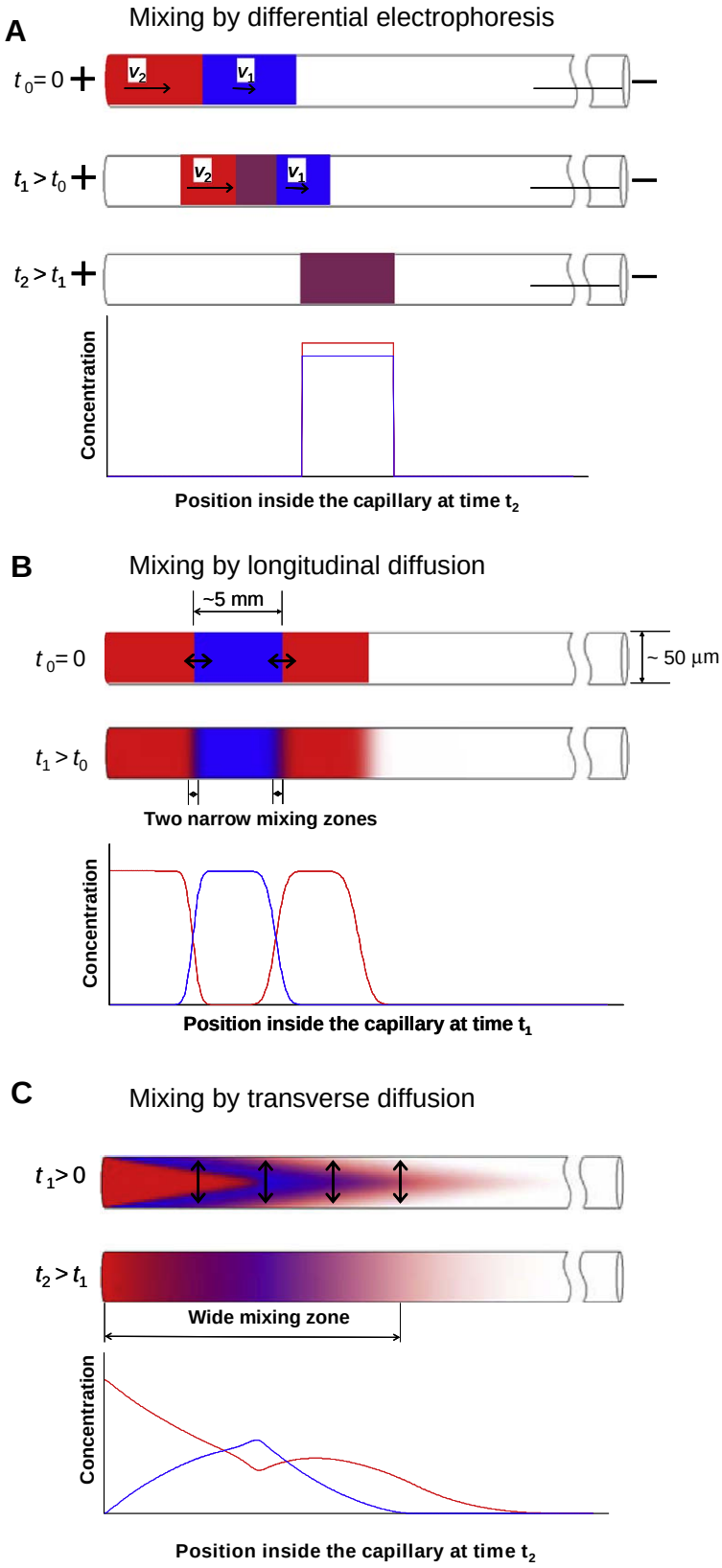

Figure 3. Mixing two reactants inside a capillary by: differential electrophoresis (**A**), longitudinal diffusion (**B**) and transverse diffusion (**C**). The illustration is out of scale and aspect ratio between plug length and diameter. In each panel, t_0 refers to the time when all reactants have been introduced, t_1 is the time for partial mixing to occur and t_2 is the time for maximum mixing. In panel **A**, v_1 and v_2 refer to the electrophoretic velocities of slower and faster reactants, respectively.

from an instrumental point of view, calculation of the concentration distribution within the capillary is more challenging. In the sections below, we describe how concentration distributions may be calculated for each mode of mixing. An Excel program is available to assist practitioners to perform these calculations.

3.1. Differential electrophoresis

Differential electrophoresis relies on different electrophoretic mobilities for the reactants to be mixed (Fig. 3A). If injection is carried out by EOF, the reactant with the lower mobility in the direction of EOF is injected first followed by the reactant with the greater mobility (Fig. 3A, upper case). When a high voltage is applied, the greater-mobility reactant moves faster than the lower-mobility reactant and penetrates the plug of the lower-mobility reactant. After some time, the plugs of the reactants can completely overlap, provided that they have identical lengths (Fig. 3A, lower case).

For mixing by differential electrophoresis, reactants can be injected by either EOF or pressure. In either case, the reactant with the lower electrophoretic mobility in the forward direction is injected first followed by the reactant with the greater electrophoretic mobility (Fig. 3, upper case). When a high voltage is applied at time t_0, the reactants start moving to the right with apparent velocities v_1 and v_2, which are values of vector sums of the corresponding electrophoretic velocities and a common electroosmotic velocity. Electric-field-driven translational movement is uniform across the capillary, which allows for very high-quality mixing by the ''ideal'' migration of the fast-reactant plug through that of the slow reactant. However, as the same translational movement moves both reactants to the distal end of the capillary, mixing is achieved away from the inlet. The distance from the capillary inlet to the rear front of the fully-overlapping plugs depends on v_1, v_2 and the plug length. Assuming that the plug lengths are identical and equal to l, we can calculate this distance to be $lv_2/(v_2 - v_1)$. Clearly, the mathematics that describes mixing by differential electrophoresis is as simple as the mathematics that describes injection by EOF.

Differential electrophoresis can produce high-quality mixing; however, the method is not generic. For instance, electrophoresis cannot be used to mix reactants with identical electrophoretic mobilities. Furthermore, if the difference in apparent reactant velocities is much less than the velocities themselves, $(v_2 - v_1) << v_2$, full mixing can only be achieved far away from the inlet and potentially near the detection end of the capillary. This situation can be reversed by applying a predetermined pulse of differential pressure to move the reaction mixture to a position close to the inlet. Time t_2 required for complete mixing is equal to $l/(v_2 - v_1)$. If this time is longer than the characteristic time of reaction, the kinetics of such a reaction can hardly be studied. Accurately predicting time of mixing is practically impossible if the reactants are dissolved in solvents with different conductivities, which is usually the case for studies of molecules prepared from biological samples (e.g., cell lysate). Finally, if more than two reactants need to be mixed, optimization of mixing becomes very tedious and highly impractical. Mixing more than two separately injected reactants by differential electrophoresis has never been reported. To conclude, mixing by differential electrophoresis is quantitative (if the solvents for different reactants are identical) but not generic.

3.2. Longitudinal diffusion

Reactants injected into the capillary by either pressure or EOF can be mixed by longitudinal diffusion. If EOF is used for injection, longitudinal diffusion is the only diffusion mode possible, since the interfaces between the plugs are strictly transverse (Fig. 3B). Longitudinal diffusion is also the only diffusion choice if low pressure is used for injection; the plug fronts are relatively flat, as are the interfaces between the plugs. Accordingly, the reactants can mix only by longitudinal diffusion.

Mixing by longitudinal diffusion is applicable to all reactants, provided diffusion is fast. However, the speed of diffusion is a limiting factor here. Time t_{diff} required for molecules with diffusion coefficient D to diffuse through a plug of length l is $t_{diff} = l^2/D$. Even for a small molecule (e.g., fluorescein, with $D = 3 \times 10^{-6}$ cm^2/s), t_{diff} through a plug with typical length of $l = 5$ mm is greater than 23 h. Diffusion through even a relatively short plug of $l = 1$ mm takes about 1 h.

In a closed reservoir of length L, the condition that the concentration approaches 0 at infinity needs to be replaced by the condition that there is no flow of material through the end of the reservoir. Mathematically, this can be written in the form of Equation (13):

$$\frac{\partial C}{\partial x} = 0, \quad x = L \tag{13}$$

This condition is satisfied if the concentration curve is considered to be reflected at the boundary, $x = L$ and the reflected curve superimposed on the original. It is reflected again at $x = 0$, then again at $x = L$, and so on. The result of each successive reflection is superimposed on the original concentration curve [6]. In a closed one-dimensional reservoir, mixing by longitudinal diffusion is described by Equation (14) [6]. The concentration C as a function of x and t is described by:

$$C(x,t) = \frac{C_0}{2} \sum_{n=-\infty}^{\infty} \left\{ erf\left(\frac{h + 2nL - x}{2\sqrt{Dt}}\right) + erf\left(\frac{h - 2nL + x}{2\sqrt{Dt}}\right) \right\} \tag{14}$$

where C_0 is the initial concentration, h is the width of the initial rectangular concentration distribution, erf is a

standard error function (equivalent to the integral of a Gaussian curve) and n is the number of reflections at the boundary. We used Equation (14) to model two reactants mixing by longitudinal diffusion (Fig. 4).

For a closed reservoir, diffusion always leads to full homogeneity of the mixed reactants. For an open reservoir, the overlap of the concentration profiles of reactants will increase with time, but full homogeneity is never reached and the shapes of the plugs change from rectangular to indefinitely broadening Gaussian (Fig. 5).

Mixing by longitudinal diffusion can be more efficient in a sandwich format, in which one reactant is surrounded by two identical plugs of another reactant (see Fig. 3B). In such a case, two mixing zones are formed, and, if the mixing time is long enough, the mixing zones can overlap. The sandwich method halves the diffusion distance for the outside reactant diffusing inwards, so it reduces mixing time by a factor of 4. Nevertheless, this does not dramatically improve the speed of mixing.

Mixing by longitudinal diffusion overcomes two limitations of mixing by differential electrophoresis. First, it can mix reactants with identical electrophoretic mobilities (e.g., neutral reactants), since diffusion is a fundamental property of all molecules. In addition, mixing by longitudinal diffusion does not result in translational movement of reactants, so the mixing zone is always near the inlet of the capillary. The rest of the capillary is therefore available for analytical separation. However, like differential electrophoresis, mixing by longitudinal diffusion is not generic. It is limited to very short plugs of small-molecule reactants and no more than two separately injected reactants.

3.3. Transverse diffusion

Mixing by transverse diffusion can occur only when the interfaces between the plugs of reactants are longitudinal [10]. Longitudinal interfaces can be formed only if reactants are injected by differential pressure high enough to inject long plugs during a short period of time to ensure that the plugs retain their parabolic shapes. However, to ensure that the flow is laminar, the pressure should not be too high. There is a large range of differential pressures that can satisfy these conditions. However, the injection time should be short enough to prevent dissipation of the parabolic profile due to transverse diffusion. To maintain laminar flow, Re should be no higher than the critical value, Re_{cr}. For a significant penetration of parabolic profiles into each other, Yo should not exceed some critical value Yo_{cr}. By combining both requirements, we can get Equation (15):

$$\mathrm{Re} = v_0 r_i/\eta = l r_i/\eta t_{inj} \le \mathrm{Re}_{cr}, \quad \mathrm{Yo} = D t_{inj}/r_i^2 \le \mathrm{Yo}_{cr} \qquad (15)$$

where l is the length of the injected plug, v_0 is the axial velocity of injection and Re_{cr} is the critical value of the Reynolds number for which the flow begins to transition from laminar flow to turbulent flow. From Equation (15), we can obtain Equation (16):

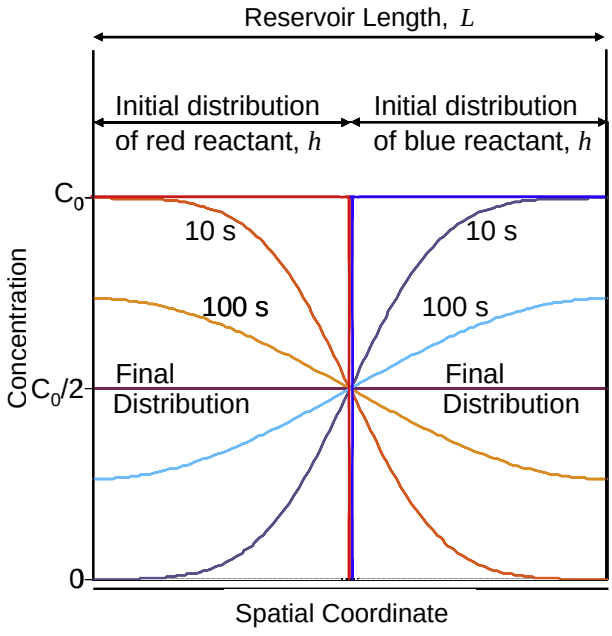

Figure 4. The change of concentration profiles of red and blue reactants in a closed reservoir caused by their longitudinal diffusion with identical coefficient of diffusion equal to $D = 5 \times 10^{-6}$ cm^2/s. The initial profiles are rectangular, occupy different halves of the reservoir and have a vertical interface in the middle of the reservoir.

$$lr_i/\eta Re_{cr} \leq t_{inj} \leq Yo_{cr} r_i^2/D \quad (16)$$

The constraint in Equation (16) can be satisfied only if the following is true [Equation (17)]:

$$l/r_i \leq Yo_{cr} Re_{cr} \eta/D \quad (17)$$

A critical value of Re for the flow in a tube is approximately 2000. A critical value of Yo is approximately 1. The viscosity of the solvent is usually higher than the diffusion coefficients of the reactants. Indeed, η is about 10^{-4} cm^2/s for water, while values of D are typically much smaller. Even for small molecules, D is typically no greater than 10^{-5} cm^2/s) and thus is an order of magnitude below η. For big molecules, such as proteins, D can be 1000 times smaller than η, so it is possible to inject a parabolic plug with a length exceeding the capillary radius by a factor of at least 2000.

Fig. 3C shows mixing by transverse diffusion of laminar flow profile (TDLFP). Conceptually, for mixing by TDLFP, solutions of reactants are injected into the capillary by differential pressure as a series of consecutive plugs. The pressure used for injection is high enough and the injection time is short enough to make the front of the laminar injection flow parabolic, so each additional plug deeply penetrates inside the previously injected plug, creating long longitudinal interfaces between them. The reactants can then be mixed by transverse diffusion through the longitudinal interfaces. Note that mixing by TDLFP contrasts dramatically with mixing by longitudinal diffusion through transverse interfaces (see Fig. 3B). To diffuse completely in the transverse direction while mixing by TDLFP, the reactant needs to diffuse a distance no greater than the inner radius of the capillary. In our typical example, depicted in Fig. 3, the internal diameter (i.d.) of the capillary is 50 μm. A fluorescein molecule, given as an example above, can diffuse through this distance in approximately 2 s. Even for a large molecule, such as a protein, with a diffusion coefficient of 10^{-7} cm^2/s, transverse diffusion takes only 1 min. Longitudinal diffusion for a molecule with $D = 10^{-7}$ cm^2/s through a 5-mm long plug would take an astonishingly long time of approximately 30 days. This example illustrates the dramatic gain in the speed of mixing when conditions are met for mixing by TDLFP.

Multiple sequentially-injected plugs will have longitudinal interfaces with neighboring plugs at a distance shorter than the capillary radius. The diffusion time required to mix multiple reactants is no longer than the time required for mixing two reactants – this time is defined by the inner radius of the capillary. In mixing by longitudinal diffusion, the diffusion distance increases with the number of reactant plugs and the diffusion time required grows as a square of the length of plugs. Thus, by contrast with longitudinal diffusion, TDLFP is suitable for mixing more than two separately-injected reactants. TDLFP satisfies the requirements for being a generic method of capillary microreactor mixing; it can facilitate fast mixing of multiple separately injected reactants of all kinds.

For TDLFP-based mixing to be quantitative, it is necessary to know concentration profiles of the mixed reactants. The following sections explain in detail the mathematics of TDLFP, which is not trivial.

3.3.1. Analytical solution. Although Equation (11) provides a general basis for the detailed modeling of plug formation and the calculation of concentration profiles of reactants in TDLFP, its analytical solution is difficult unless simplifying assumptions are made. Solving Equation (11) analytically becomes possible if either of the two terms on the right side of the top equation is negligible with respect to the other. In the other words,

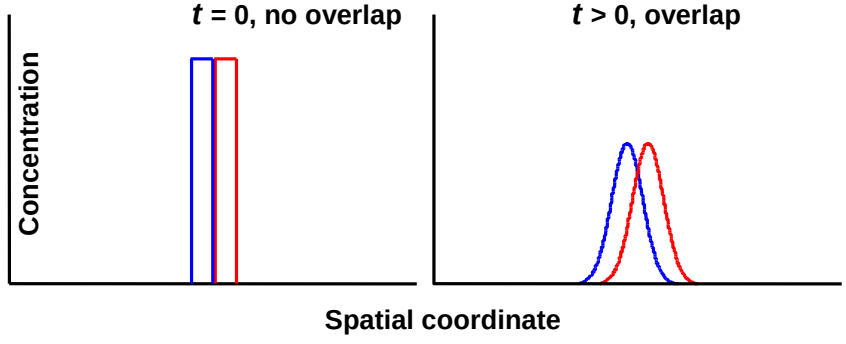

Figure 5. Simulation of the mixing of red and blue reactants by longitudinal diffusion with the same diffusion coefficients inside an open capillary. The initial concentration profiles (for $t = 0$) are rectangular and have no spatial overlap. At time $t > 0$, the reactants diffuse with a growing spatial overlap. However, By contrast to the closed reservoir, the shape of the profiles will never again be rectangular; it will always be broadening Gaussian.

the analytical solution of Equation (11) can be found if either:

(i) Yo is assumed to be zero (this assumption is equivalent to assuming that either the transverse diffusion is negligible during the injection or the injection time is much shorter than the characteristic time of transverse diffusion); or,

(ii) the velocity is assumed to be zero (this assumption is satisfied during the vial change between the injections of different reactants).

If the assumptions are used separately, they are experimentally ''meaningful''. The assumption of negligible diffusion during injection simplifies Equation (11) to Equation (18):

$$\frac{\partial c}{\partial \tau} = -\omega(\tau)(1-\rho^2)\frac{\partial c}{\partial \chi} \tag{18}$$

Equation (18) describes the plug formation during the injection and has the general solution in Equation (19):

$$\begin{aligned} \lambda &= \int_{\tau_0}^{\tau} \omega(\tau')d\tau' \\ c &= F(\chi - (1-\rho^2)\lambda) \end{aligned} \tag{19}$$

where τ' is an internal parameter of integration and λ is the dimensionless length of the injected plug, which is positive for a positive injection velocity ($\omega > 0$). If the reactant plug is injected from a vial, in which the concentration of the substance is C_{max}, the distribution of the concentration inside the capillary is described by the Equation (20):

$$c(\tau, \chi, \rho) = \theta(\chi - (1-\rho^2)\lambda) \tag{20}$$

Here, $\theta(\chi)$ is a function that equals 1 if $\chi > 0$ and 0 otherwise. This function allows one to describe the distribution of the substance not only after but also prior to the injection ($\tau < \tau_0$). According to Equation (20), if $\chi < 0$, the concentration of the substance inside the capillary ($\chi > 0$) is zero. At the interface between the capillary and the solution in the vial ($\chi = 0$), the concentration of the substance is equal to that in the vial. According to Equation (20), the profile of the injected plug is parabolic.

Inside the capillary, the dimensionless concentration $c = C/C_{max}$ equals 1 within the plug and 0 outside the plug. Knowing the shape of the plug allows calculation of the average dimensionless concentration for each section of the capillary, following Equation (21):

$$\tilde{c}(\tau, \chi) = 2\int_0^1 c(\tau, \chi, \rho)\rho d\rho \tag{21}$$

where $\tilde{c}$ describes the average dimensionless concentration for a particular section of the capillary.

In particular, for the parabolic distribution described by Equation (21), the average ''per-section'' concentration is reached once the reactant diffuses in the transverse direction for a time longer than r_i^2/D. Equation (22) may be used to calculate $\tilde{c}$:

$$\tilde{c}(\chi) = \theta(\lambda - \chi)(1 - \chi/\lambda) \tag{22}$$

The χ-profile of this distribution is linear.

Generally, when multiple plugs of different reactants are injected, some time is needed to change the vials. This time cannot be less than a few seconds, meaning that the assumption of no transverse diffusion during the vial switch may be unreasonable for small molecules. If the assumption of no transverse diffusion cannot be made, Equation (11) needs to be solved for diffusion with the single assumption of no translational movement between injections. If we assume that $\omega = 0$, Equation (11) can be simplified to the system of equations in Equation (23):

$$\begin{aligned} &\frac{\partial c}{\partial \tau} = \mathrm{Yo}\frac{1}{\rho}\frac{\partial}{\partial \rho}\rho\frac{\partial c}{\partial \rho} \\ &\left.\frac{\partial c}{\partial \rho}\right|_{\rho=1} = 0 \end{aligned} \tag{23}$$

As mentioned above, if the reactant(s) is/are allowed to diffuse in the transverse direction for a time no shorter than r_i^2/D, then the average concentration will be reached throughout the cross-section according to Equation (22). The assumption of ''complete'' transverse diffusion can be easily achieved experimentally by allowing long enough time (longer than r_i^2/D and shorter than l^2/D) for all reactants to diffuse in the transverse direction between plug injections. As a result, all radial concentration gradients will be eliminated for all injected plugs.

3.3.2. Simulation of TDLFP using the analytical solution. The analytical solution of Equation (11) developed in sub-section 3.3.1 can facilitate simulation of TDLFP-based mixing and calculation of reactant-concentration profiles using different sets of simplifying assumptions.

Here, we present simulation of TDLFP under two sets of simplifying assumptions. The first simulation is for mixing three reactants while assuming that:

(i) longitudinal diffusion is negligible at all times; and,

(ii) transverse diffusion is negligible during plug injections and starts only after the injection of the last plug.

The second assumption is very stringent but can be experimentally fulfilled when mixing large molecules, such as proteins. Fig. 6A illustrates the steps of mixing, using the above two assumptions and the resulting concentration profiles of the three mixed reactants calculated using the analytical model [Equations (18)–(23)]. The five steps of simulated mixing are as follows. In the first three steps, identical plugs of the three reactants are injected. In Step 4, a blank buffer is injected to increase the length of longitudinal interfaces and,

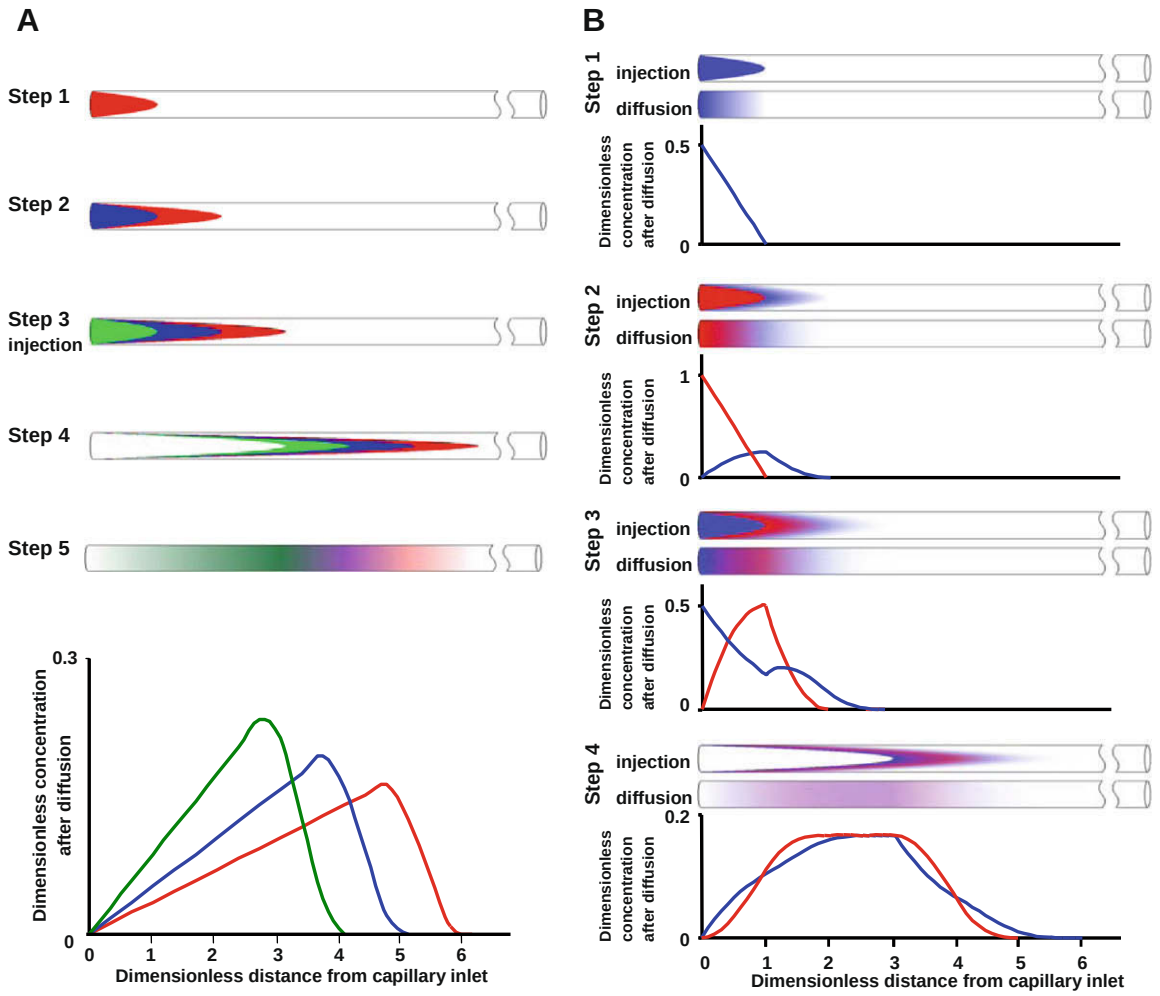

Figure 6. Simulated TDLFP-based mixing of reactants inside the capillary. (**A**) Three reactants (red, blue, and green) are mixed, assuming that there is no diffusion until the last plug is injected and that there is only transverse diffusion after the last plug is ingested. (**B**) Two reactants (blue and red) are mixed in sandwich mode, assuming no longitudinal diffusion at any time, no transverse diffusion during the injection of every plug, and complete transverse diffusion between plug injections. The white color inside the capillary corresponds to pure solvent. The graphs show the simulated concentration profiles of the reactants along the capillary after corresponding steps of mixing. The colored plugs have identical volumes; the volume of the last (white) plug is equal to the sum of the volumes of all colored plugs.

thus, increase the level of their spatial overlap. Finally, the reactants are allowed to diffuse in the transverse direction. The result of the simulation presented in Fig. 6A demonstrates that TDLFP-based mixing leads to a significant spatial overlap of the three reactants near the inlet of the capillary.

The analytical solution of Equation (11) was also used to simulate the mixing of two reactants in a sandwich mode with three simplifying assumptions (Fig. 6B). The three simplifying assumptions used to obtain Equation (17) analytically are:

(i) negligible longitudinal diffusion during the entire mixing procedure;
(ii) negligible transverse diffusion during single plug injection; and,
(iii) a long waiting period between plug injections to allow for transverse diffusion to eliminate any gradients of reactant concentrations in the transverse direction.

The procedure is performed in four steps. First, a 1 mm-long plug of the first reactant is injected and allowed to diffuse in the transverse direction. Second, the second reactant is injected penetrating into the plug of the first reactant, and the two reactants are allowed to diffuse in the transverse direction. Third, to improve the quality of mixing, an additional plug of the first reactant is injected and the reactants are allowed to diffuse in the transverse direction. Finally, to improve the overlap of the mixed solutions further, a plug of a pure buffer is injected and the reactants are allowed to diffuse in the transverse direction to reach the final concentration profiles depicted in the lower graph in Fig. 6B. It is important to emphasize that the quality of mixing that results is much better than one can obtain from

longitudinal diffusion through transverse interfaces. Furthermore, the sandwich configuration provides a greater level of spatial overlap than the standard sequence configuration depicted in Fig. 6A.

3.3.3. Numerical solution. Although the analytical solution of Equation (8) is instructive for the qualitative study of TDLFP-based mixing, it depends on the assumption of no diffusion during the injection of individual plugs, the assumption used to obtain simplified Equation (11). This assumption is too stringent for the analytical model to be generic.

For small molecules, transverse diffusion during the injection may be significant, making the model inaccurate, so it cannot be used for quantitative applications, which require knowledge of the concentration profiles of the mixed reactants. Therefore, if the mixing process involves small molecules, the analytical solution of Equation (8) cannot be found and a numerical approach must be used to solve it.

We describe here a special case of Equation (8), which corresponds to injection by a constant differential pressure. In this case, the flow velocity is also constant during the injection: $w = 1$. To facilitate the solving of Equation (8) numerically, the equations are presented in the following form [Equation (24)]:

$$\frac{\partial c}{\partial \tau} = -(1-u)\frac{\partial c}{\partial \chi} + 4\mathrm{Yo}\frac{\partial}{\partial u}u\frac{\partial c}{\partial u}$$
$$\left.\frac{\partial c}{\partial u}\right|_{u=0} = 0, \qquad \left.\frac{\partial c}{\partial u}\right|_{u=1} = 0 \tag{24}$$

A new variable, $u = \rho^2$, is introduced here. When numerically modeling Equation (24), it is preferable to use an algorithm that does not distort concentration profiles in the absence of diffusion. Every iteration step in such a computation comprises two sub-iterations. In the first sub-iteration, the process of longitudinal plug shift is modeled, assuming no transverse diffusion. In the second sub-iteration, transverse diffusion is modeled without a longitudinal shift of the plug. The first sub-iteration is designed to average out the error in the modeling of longitudinal shifts after a large number of iterations. In the second sub-iteration, a numerically stable scheme of computation is used. Computational modeling is performed for a uniform three-dimensional grid with axes T, Y, and U, incremental steps Δt, Δy, and Δu, and lengths from zero to T, Y, and U, respectively. The resulting computational scheme is presented below [Equation (25)]:

$$c^{T+\frac{1}{2}}_{Y+Dy_{T,U},U} = c^{T}_{Y,U}$$

$$\frac{c^{T+1}_{Y,0} - c^{T+\frac{1}{2}}_{Y,0}}{\Delta t} = \left(\frac{2\mathrm{Yo}}{\Delta u^2}\right)(c^{T+1}_{Y,1} - c^{T+1}_{Y,0})$$

$$\frac{c^{T+1}_{Y,U} - c^{T+\frac{1}{2}}_{Y,U}}{\Delta t} = \left(\frac{4\mathrm{Yo}}{\Delta u^2}\right)\begin{bmatrix}(U+\frac{1}{2})c^{T+1}_{Y,U+1}+\\(U-\frac{1}{2})c^{T+1}_{Y,U-1}-\\(2U+1)c^{T+1}_{Y,U}\end{bmatrix}, \quad 0 < U < \tilde{U}$$

$$\frac{(c^{T+1}_{Y,\tilde{U}} - c^{T+\frac{1}{2}}_{Y,\tilde{U}})}{\Delta t} = \left(\frac{4\mathrm{Yo}}{\Delta u^2}\right)\left(\tilde{U}-\frac{1}{2}\right)(c^{T+1}_{Y,\tilde{U}-1} - c^{T+1}_{Y,\tilde{U}}) \tag{25}$$

where shifts along the capillary axis, $Sy_{T,U}$, are calculated using the following algorithm [Equation (26)]:

$$Sy_{T,U} = round\left\{\left[(1-U\Delta u)T\Delta t - \sum_{T'=0}^{T'=T-1} Sy_{T',U}\right]/\Delta y\right\} \tag{26}$$

In Equation (26), *round*, a function of rounding to the nearest integer is used. Variables in Equation (25) are related to the discrete variables in Equation (25) and Equation (26) in the following way [Equation (27)]:

$$\tau = T\Delta t, \quad \chi = Y\Delta y, \quad u = U\Delta u \tag{27}$$

In addition, the following equality is fulfilled [Equation (28)]:

$$\tilde{U}\Delta u = 1 \tag{28}$$

The above computational procedure can be adopted by any researcher with computational experience (e.g., using Excel Solver).

Several versions of software were designed to simulate TDLFP in Excel (as a flexible interface) and Object Pascal [as a DLL library, containing calculations which were based on Equation (24)]. The most recent versions of the software have been published in the Research section of the following web page: www.chem.yorku.ca/profs/krylov.

There are two versions of the software interface that can be downloaded from the site. One version of software calculates concentration profiles of TDLFP-mixed reactants as an intermediate step in the determination of K_d in the formation of aptamer-protein complex. The other version calculates concentration profiles of an arbitrary number of reactants mixed by TDLFP but does not have options for modeling the reaction kinetics. Both versions have a detailed Help option.

3.3.4. Simulation of TDLFP using the numerical solution. Using the above computational approach, TDLFP-facilitated mixing of three reactants was simulated and studied under different conditions. In particular, there was a study of the influences of Yo, the length of the terminating solvent plug, ''shaking'' and double injection on the quality of TDLFP-facilitated mixing of three reactants. Fig. 7 shows the final distributions of the three reactants over the capillary length for the different scenarios of mixing. The order of reactant injection is: red, blue, and then green. For each diagram, Yos of the three reactants were assumed identical and the injected

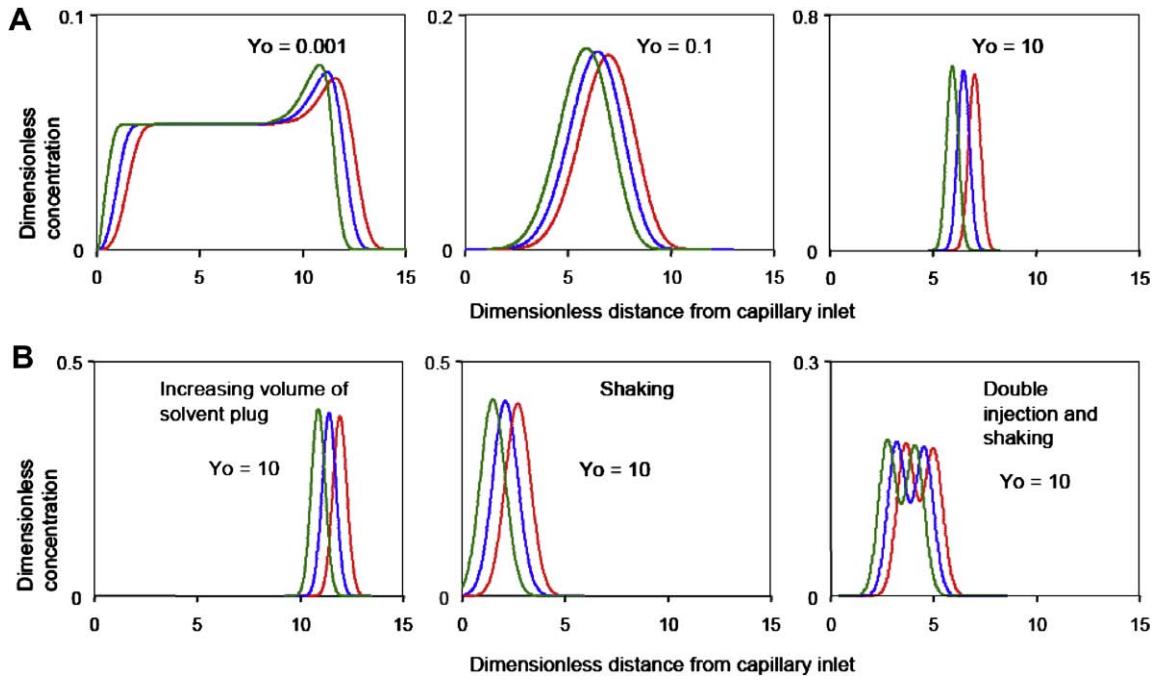

Figure 7. (**A**) Numerical simulation of TDLFP-based mixing of three reactants with different York numbers (Yo) and (**B**) different scenarios of mixing for the same York number. The graphs show the concentration profiles of red, blue, and green reactants after simulated mixing. In each diagram, the York numbers of the three components are identical. In Panel **A**, the simulation was performed for identical volumes of the red, blue, and green components, followed by a terminating plug of solvent with a volume four times the cumulative volume of the three injected reactants. In Panel **B**, the improvement in the quality of mixing is demonstrated by: increasing the volume of the terminating solvent plug by a factor of 7/4 (left); using a ''shaking'' approach achieved by applying a reverse pressure pulse with duration and amplitude similar to that used for the injection of the terminating buffer plug (middle); and, using double injection combined with the ''shaking'' approach, in which the injection of the three reactants is repeated with half concentrations, followed by injection of a solvent plug and ''shaking'' (right).

volumes of the reactants were also identical. A terminal solvent plug of a volume 4 or 7 times the cumulative volume of the three reactant solutions is injected after the green reactant. This final injection plays an important role in improving the uniformity of the mixed reactants, leading to better mixing. The time between injections of individual plugs is assumed to be long enough for the transverse diffusion to create complete uniformity of all reactants throughout the capillary cross-section. The quality of mixing is judged visually by the spatial overlap of the concentration profiles.

Results show that the mixing can be efficient only with a sufficiently low Yo (Fig. 7A). The quality of mixing decreases with increasing Yo. This decrease becomes very significant when the value of Yo exceeds 1 (Fig. 7A, right). Low quality of mixing is attributed to fast transverse diffusion during the injection, preventing the formation of the needle-like structure of the injected plug and decreasing the efficiency of the inter-penetration of the mixed solutions. One way to improve the quality of mixing is to decrease Yo by decreasing the injection time [see Equation (12)]. Decreasing the injection time, while keeping the injected volume constant, can be difficult due to the hydrodynamic inertia. However, commercially available instrumentation makes it possible to generate short pulses (<1 s) at a suitably high pressure (>3 psi) to inject sufficiently long (>1 mm) plugs of solutions very quickly. Hence, Yo can be significantly decreased even for reactants with large diffusion coefficients.

Another way to improve the quality of mixing is to increase the volume of the solvent plug in the final step (Fig. 7B, left). Although increasing the length of the solvent plug decreases reactant concentration through dilution and lowers kinetic rates in concentration-dependent reactions, the dilution factor can be calculated by the mathematical models described above. This advantage allows for the initial pre-injection concentration at which the desirable kinetics is achieved to be found a priori. One of the drawbacks of increasing the volume of the pure solvent plug is that the solution plugs travel further from the inlet of the capillary, decreasing the separation efficiency in the following step of microanalysis. Moreover, if the injected pure solvent differs from the separation buffer, the separation conditions may be significantly altered.

To overcome these problems, a ''shaking'' method, in which a series of negative and positive pressure pulses are applied to the capillary inlet after the final solvent plug, can be used [11]. The negative pressure reverses the parabolic profiles and improves the quality of mixing. The alternating backward and forward movements

repeat this improvement and are somewhat analogous to mechanical shaking. The simulation shows that the quality of mixing for the ''shaking'' approach is comparable to the one with an increased volume of terminating solvent plug (Fig. 7B, left and middle). In the left graph of Fig. 7B, the terminating plug was 7/4 longer than that in the other graphs. While the effects of the longer terminating plug and shaking are similar, shaking has the advantages of decreased dilution of reactants and smaller volumes occupied by the mixture.

Further improvement of mixing quality can be achieved by combining the shaking approach with double injection, in which each reactant is injected separately twice with half the concentration in each injection. For instance, after consecutive injection of the three reactants into the capillary with half concentrations, each reactant is injected again in the same order and with the same concentrations. Combining the shaking approach with double injection significantly improves the quality of mixing without injecting a relatively long solvent plug (Fig. 7B, right) even in the case of a large Yo.

4. Reaction

When mixed together, the reactants will react on their own if conditions, such as temperature and concentrations, are suitable. For every specific reaction, this step is fully specified by the reaction and is thus generic.

The second criterion, that the step be quantitative, still needs to be considered. For the reaction step to be quantitative, mathematics is needed to calculate the kinetics in a non-homogeneous mixture. The mathematical apparatus for quantitation is described below in Section 6; however, here we describe some considerations related to reaction conditions. If the conditions are chosen so that the reaction proceeds to a great extent during the mixing, quantitation (in the sense of finding rate constants) will require the combined modeling of reaction kinetics and mixing. This is obviously not a trivial task. The procedures of calculation can be significantly simplified if reaction conditions are chosen so that the reaction does not proceed far from the initial conditions during mixing. In this case, product formation during mixing can be neglected and the kinetics can be calculated assuming no mass transfer. If needed, the reaction rate can be reduced by decreasing the concentrations of reactants. If this cannot be done, an attempt to decrease the mixing time can be made. Thus, one desirable condition is that the characteristic mixing time is much shorter than the characteristic reaction time.

Another consideration to simplify the mathematics is to have identical reaction conditions (e.g., temperature, pH and buffer concentration along the entire length of

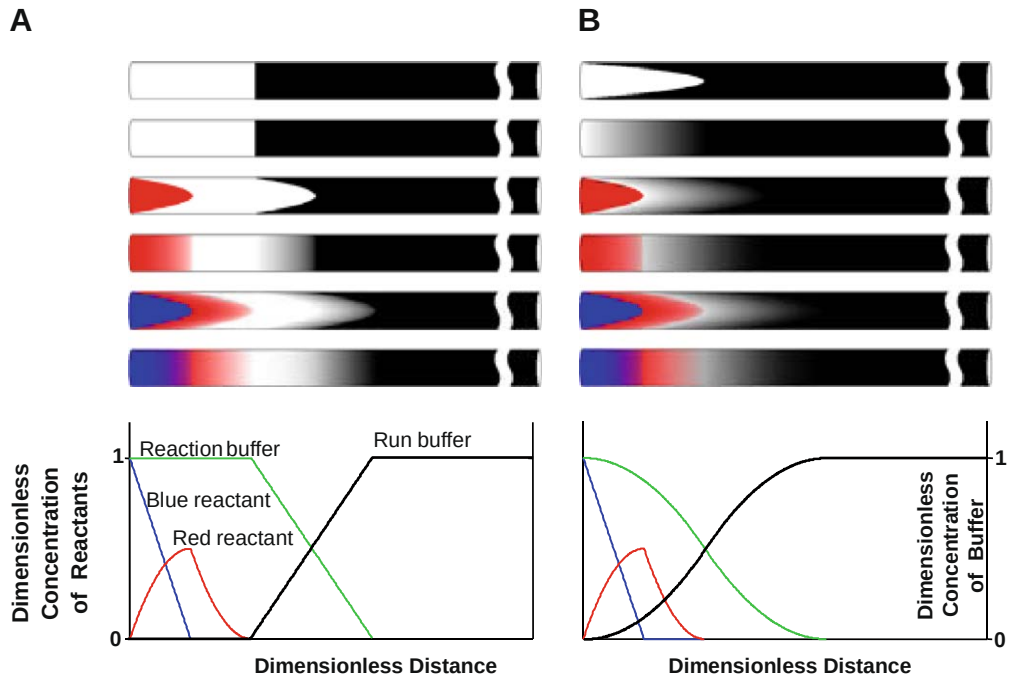

Figure 8. Effect of the separator-plug shape on the mixing of the run buffer with the reactants in the reaction zone. The white area corresponds to the reaction buffer and the black area to the run buffer. **Panel A** illustrates a case of a rectangular separator plug that can be injected by electroosmotic flow (EOF) or by low pressure that corresponds to Yo >> 1. In this case, the reaction mixture is isolated from the run buffer. **Panel B** corresponds to a parabolic separator plug that occurs when the plug is injected by pressure, which corresponds to Yo $\leqslant$ 1. Transverse diffusion enables the run buffer to intrude into the reaction zone.

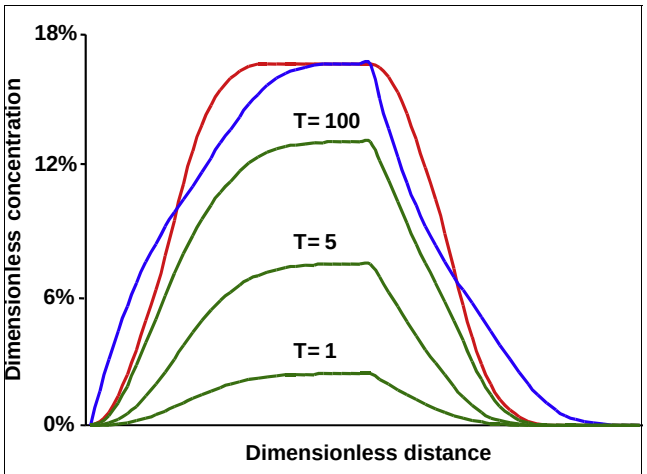

Figure 9. Progress of product (green) formation with time for a binary reaction of red and blue reactants mixed by TDLFP. The rate constants of the forward and backward processes are k_1 and k_2, respectively. The red and blue traces show the concentrations of reactants just after mixing, $t = 0$. Parameter T is equal to $t \times k_1 \times C_{inj}$, where t is time, k_1 is the binding-rate constant and C_{inj} is the concentration of injected red reactant at the inlet of the capillary. The green plots show the concentration of the product as a function of T. The reciprocal equilibrium constant, $1/K_{eq} = k_2/k_1$, is assumed to be equal to 1% of C_{inj}.

the reaction mixture). While temperature is easy to keep constant along a relatively short (~1-cm plug of the reaction mixture), other conditions may be more difficult to control in the case when the run buffer and the reaction buffer do not match. This situation occurs, for example, when reactants involve sensitive molecules (e.g., proteins) and the quality of separation in the next step of IMReSQ requires the presence of a denaturing agent (e.g., surfactant) in the run buffer. Whether or not this problem can be solved depends on the methods for injecting reactants and mixing. For example, if the reactants are mixed by an electric field, it is hard to preclude the run buffer from mixing with the reactants. By contrast, when reactants are mixed by diffusion, the reaction mixture can be prevented from mixing with the run buffer by introducing a ''separator'' plug of the reaction buffer prior to injecting the first reactant (see Fig. 8).

For a separator plug to work efficiently, it must have a rectangular rather than a parabolic profile (Fig. 8A). It can be achieved by either injecting the separator plug by EOF or injecting it by low enough pressure to ensure that Yo >> 1. The minimum length of such a rectangular separator plug should be no less than the distance from the capillary inlet to the front of the reaction zone (the zone where all reactants are present). If the separator plug is pressure-injected with low values of Yo, it will have a parabolic shape and will be mixed with the reactants in the reaction zone (Fig. 8B).

The main process in this stage of the IMReSQ procedure is the reaction of the reactants; we can neglect longitudinal mass transfer and describe the reaction for every capillary cross-section separately, assuming homogeneous distribution of the reactants and products through the cross-section. In each cross-section, the concentrations of reactants and products will be heading towards the local equilibrium. How close the final concentrations will be to equilibrium will depend on the reaction time. Fig. 9 illustrates the result of such a consideration for a binary reaction of two reactants (red and blue) forming a single product (green).

5. Separation

There is no generic separation approach in IMReSQ. The separation method of choice depends on the kinds of reactants and products to be separated. In general, the capillary format is compatible with two major separation methods: CE and capillary electrokinetic chromatography [CEKC, also called capillary electrochromatography (CEC)]. We do not consider classical capillary chromatography, as it typically uses columns of a relatively large i.d. of approximately 100–500 μm, contrasting with CE and CEC that utilize capillaries with i.d. of 20–75 μm. Within every method, there is a variety of modes that provide a great level of flexibility that practically guarantees that, for every reaction, a method or mode can be found to separate the products and the reactants of interest, so separation is fundamentally a non-generic step.

The choice of the separation mode will depend not only on the nature of reactants and products but also on the methods of injecting and mixing reactants. CE as a separation method is compatible with all methods of injecting and mixing reactants. In CEC, the capillary is filled with a stationary phase that creates significant resistance to pressure-driven injection and makes the hydrodynamics of pressure-driven flow differ from those in an open capillary. It is much more difficult to generate high-quality parabolic profiles in a packed capillary, so mixing by TDLFP is hardly compatible with CEC.

However, CEC is compatible with injection or mixing using an electric field. To be quantitative, the reactants and the products of interest need to be baseline separated so that their quantities can be accurately determined. If separation of the reactants and the products from the reaction mixture into separate zones is fast in comparison to the characteristic reaction time, no additional mathematics needs to be used.

However, if the reaction proceeds to a considerable extent during the separation, mathematics needs to be developed to solve for the reaction kinetics in the presence of the separation-induced mass transfer along the capillary. In general, numerical methods are used to solve this case. There are many effective approaches for

smooth concentration distributions. However, in electrophoretic separations, we often deal with sharp peaks and fronts; this dictates the need to use specific numerical algorithms. One of the simplest ways is to use special discrete approximations, for which errors of numerical solutions do not increase with time. For a single reactant, computational modeling is performed using a uniform 2-dimensional grid with axes T and X and incremental steps Δt and Δx. The simplest computational scheme utilizing this approach for the electrophoretic mass transfer is presented in Equation (29):

$$\frac{c_X^{T+1} - c_X^T}{\Delta t} = -v\frac{c_X^T - c_{X-1}^T}{\Delta x} \quad (29)$$

where c is the dimensionless concentration of the reactant. According to Equation (29), in the next iteration with respect to time, the concentration will be as in Equation (30):

$$c_X^{T+1} = \left(1 - v\frac{\Delta t}{\Delta x}\right)c_X^T + v\frac{\Delta t}{\Delta x}c_{X-1}^T \quad (30)$$

so that the dimensionless concentration at any location is derived from the previous concentrations in the immediate vicinity and accounts for peak broadening. Equation (30) incorporates the effect of additional pseudo-diffusion, which is not connected with physical diffusion. If Equation (31) is satisfied:

$$\Delta x = v\Delta t \quad (31)$$

the concentration at a particular coordinate X will depend only on the previous concentration at coordinate $X - 1$, and there will be no pseudo-diffusion but only an axial displacement (i.e. $c_X^{T+1} = c_{X-1}^T$).

In other words, the reactant is simply transported along the capillary. However, when the reaction continues during the separation, the simple model described in Equations (29)–(31) will introduce small errors.

6. Quantitation

When the reactants and the products are separated, those of interest need to be detected and quantitated. Several detection methods, can be easily interfaced with capillaries [e.g., optical (fluorescence and absorbance) [12]], amperometric and conductivity detection [13], and mass spectrometry (MS). Each of them can be used to determine the amounts of separated reactants and products accurately. Fluorescence is the method with the lowest limit of detection (LOD); it can detect single molecules of the analyte if an appropriate fluorophore is present [14]. However, most molecules are not fluorescent. There have been attempts to label molecules with fluorescence, but they are not generally applicable. For example, fluorescent labeling can rarely be applied to small molecules.

Light absorption is a more generic method than fluorescence. All molecules absorb light in one spectral region or another. However, light absorption has a relatively high LOD due to a short optical path-length in the narrow-bore capillaries.

Amperometric detection is limited to redox-active molecules, so it is not generic; however, its LOD can be as low as that of fluorescence detection [15].

Capacitatively-coupled contactless conductivity detection is a generic detection methods, but its LODs tend to be greater than 100 nM [16], and optimization for sensitivity tends to produce triangular peaks with a resulting decrease in resolution. LODs are even higher for neutral species that require indirect detection [17].

MS is a generic detection method that can detect virtually all molecules. The LOD of MS is still no match to those of fluorescence or amperometric detection, but it is better than that of light absorption. Optical and electrochemical detections are quantitative [17], while MS can be made quantitative only if an internal standard with the ionization efficiency identical to that of the analyte is used.

Typical detector data contain signal, background offset (systematic error) and noise (random errors). For data processing, it is necessary to know the characteristics of the noise. The simplest model for noise is that its amplitude follows a normal or a Poisson distribution (when the parameter being measured can take only positive values). It is also assumed that the amplitude of the noise at any moment in time is independent of the amplitude at any other time. These assumptions are not always perfectly satisfied. Indeed, in real experiments, the background level and hence the systematic error can drift and noise often correlates for experimental measurements taken in quick succession – typically described as a lag effect. Nevertheless, the simplest noise model is often satisfactory. When a model is fitted to experimental data, Y_i^e, the sum of the squares of the Euclid distance between the data and model (d) can be used as a measure of the accuracy of the fit, the smaller the value of d, the better the fit [Equation (32)]:

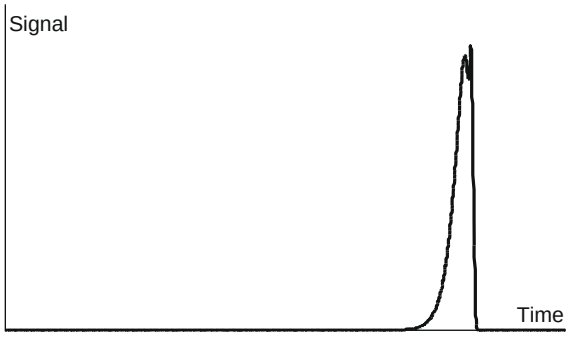

Figure 10. Sample of modeled dynamics of two-stage decay.

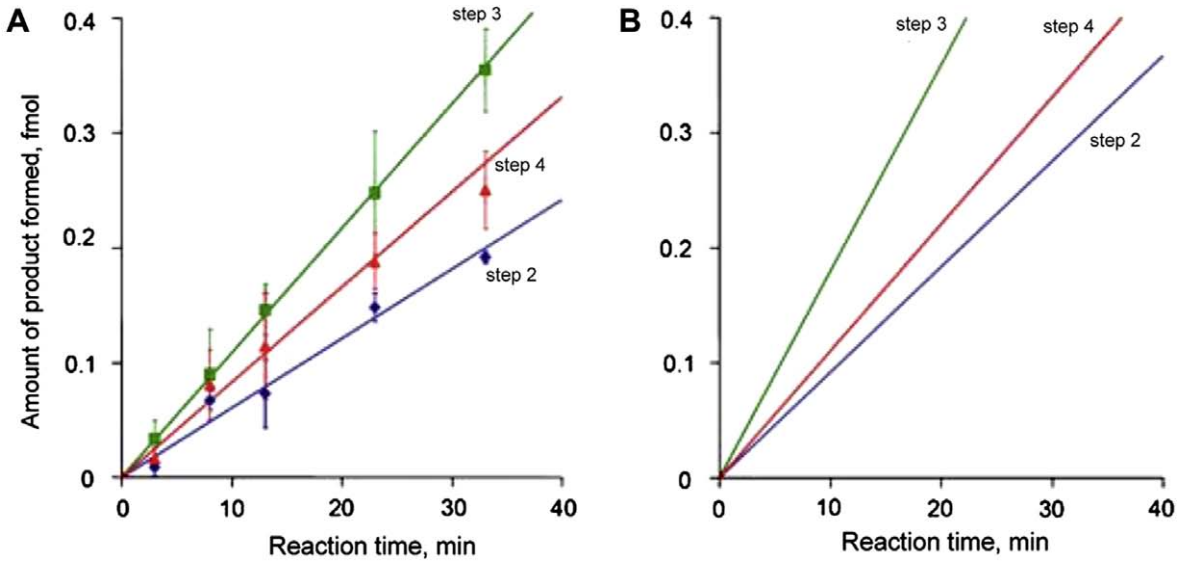

Figure 11. Experimental (**A**) and simulated (**B**) kinetics of enzymatic glycosylation of fluorescein-mono-β-D-galacto-pyranoside. The enzyme and the substrate were mixed by TDLFP using a procedure depicted in Fig. 6**B**. The simulated kinetics was calculated by integrating product formation along the capillary length using experimental values of K_m and k_{cat} (Reprinted with permission from [20], © 2005 American Chemical Society).

$$d = \sum_i (Y_i^m + bg - Y_i^e)^2 \qquad (32)$$

where Y_i^m is the modeled data that corresponds to Y_i^e and bg is the background offset. The noise model chosen also depends on the way that the data are presented. For example, if a Gaussian model of noise is applicable for the initial data, Y_i^e, this model will not be applicable for values of $(Y_i^e)^2$ and it would be inappropriate to use Equation (32) to measure the accuracy of the fit.

For accurate quantitation, it is essential that electropherograms are correctly interpreted. For example, the simulated electropherogram shown in Fig. 10 could be interpreted as the superposition of two peaks of stable molecules with very similar electrophoretic mobilities.

In reality, it was simulated from a two-stage fast dissociations of a complex, with electrophoretic mobility approximately double that of its stable product of decay. Equation (33) for the reaction is shown below:

$$AB_2 \rightarrow AB + B \rightarrow A + 2B \qquad (\mu_{AB} \simeq 2\mu_A) \qquad (33)$$

The sharp peak in Fig. 10 is due to free **A**, present at the start of the reaction; the wider peak is due to **A** formed from the 2-stage dissociation of $\mathbf{AB_2}$.

7. Experimental implementation of IMReSQ

7.1. Electrophoretically-mediated micro-analysis

There are two original modes of IMReSQ that are historically called electrophoretically-mediated micro-analysis (EMMA). The first mode utilizes an electric field for both injection of reactants into the capillary and mixing them inside the capillary [18]. It was only used for injection and mixing of two separate plugs of solutions due to the restrictions, outlined in Sections 2 and 3.

When three reactants are to be mixed (e.g., enzyme, substrate, and inhibitor), two of them must be pre-mixed in a vial outside the capillary [18]. The second experimentally-proved mode of EMMA uses pressure for reactant injection and longitudinal diffusion to mix the reactants [19]. While this mode overcomes some limitations of the first one, longitudinal diffusion is so inefficient that it cannot mix more than two separately injected solutions. Due to this restriction, this mode did not find practical application beyond proof of principle.

Examples of applications of the two modes have been well reviewed in recent years [19]. However, it is important to mention that these two modes have never been used for the determination of rate constants of chemical reactions.

7.2. TDLFP-based IMReSQ

The third experimentally-proved mode of IMReSQ utilizes injection by pressure and mixing by TDLFP. TDLFP-based IMReSQ was first demonstrated in 2005 [20] and has rarely been reviewed [11], so we describe here the major experimental advances for this mode.

7.2.1. Mixing of two reactants. The first experimental proof of TDLFP mixing was demonstrated with two reactants: enzyme β-galactosidase and substrate fluorescein-mono-β-D-galactopyranoside [20]. β-galactosidase catalyzes the hydrolysis of this substrate with the release of fluorescein. Enzyme and substrate were mixed using a scheme shown in Fig. 6B. The order of the four plugs was: substrate, enzyme, same substrate and

solvent (buffer solution). After mixing, the enzymatic reaction was allowed to proceed for varying periods of time. The reaction was stopped by electrophoretically separating the enzyme from the substrate; the product (fluorescein) was also electrophoretically separated from the unreacted substrate. Due to the high efficiency of CE, this separation takes no longer than a few seconds. This time is much shorter than the time required for TDLFP-based mixing, so it can be ignored in the overall calculation. The quantity of the product was measured with a fluorescence detector at the distal end of the capillary. It was found that the enzymatic reaction was time dependent and concentration dependent, so confirming that the reactants were mixed.

Next, the experimental reaction kinetics was compared with the kinetics predicted by the analytical TDLFP model. The simulated kinetics was calculated by integrating product formation along the capillary length. This model used the values of the catalytic rate constant, k_{cat}, and the Michaelis constant, K_m, which were determined in a separate experiment by mixing the reaction components in a vial.

Fig. 11 compares experimental and simulated reaction kinetics for 2-, 3-, and 4-step mixing procedures described in Fig. 6B. The initial reaction rates in the experiment agreed not only qualitatively but also quantitatively. The simulated reaction rates for steps 2, 3, and 4 were greater than the experimental ones by a factor of approximately 1.5. This difference between experimental and simulated rates is most likely to be due to the model not taking into account transverse diffusion during plug injection. This result demonstrated that two reactants can be efficiently mixed using TDLFP. The result also suggested that accurate quantitative prediction of the reaction rate requires more accurate modeling of TDLFP (which takes into account diffusion during injection); this can only be achieved numerically.

Recently, TDLFP mixing of two reactants was used to facilitate the determination of the equilibrium-dissociation constant of an affinity complex between a protein and a DNA aptamer [1]. A DNA aptamer is a single-stranded DNA oligonucleotide capable of binding its affinity target with high selectivity and affinity. Aptamers are selected from large libraries of random DNA sequences (10^{12}–10^{15} different sequences) by using an affinity method. KCE is a conceptual platform for the development of affinity methods that can, in particular, be used for highly efficient selection of DNA aptamers. Selection of aptamers with KCE methods can be achieved with only a few rounds and, thus, leads to highly-diverse pools of aptamers. Screening a large number of candidate aptamers for their affinity to the target protein is a challenging task. Screening affinity of an aptamer for the target protein in a capillary for integrated microanalysis promises to make high throughput easier and to minimize consumption of the protein.

TDLFP was used as a mixing method for a proof-of-principle work on integrated microanalysis for measuring the affinity of aptamers [1]. Experimentally, TDLFP mixing of the aptamer and its target protein was achieved using a scenario similar to that described in the β-galactosidase example above and depicted in Fig. 6B. After mixing, the protein and the aptamer were allowed to react and to form a protein-aptamer complex. The incubation time was long so that equilibrium would be approached. The complex was then separated from the unreacted aptamer and both the complex and the unreacted aptamer were quantitated fluorescently using a fluorescein dye that was covalently linked to the aptamer.

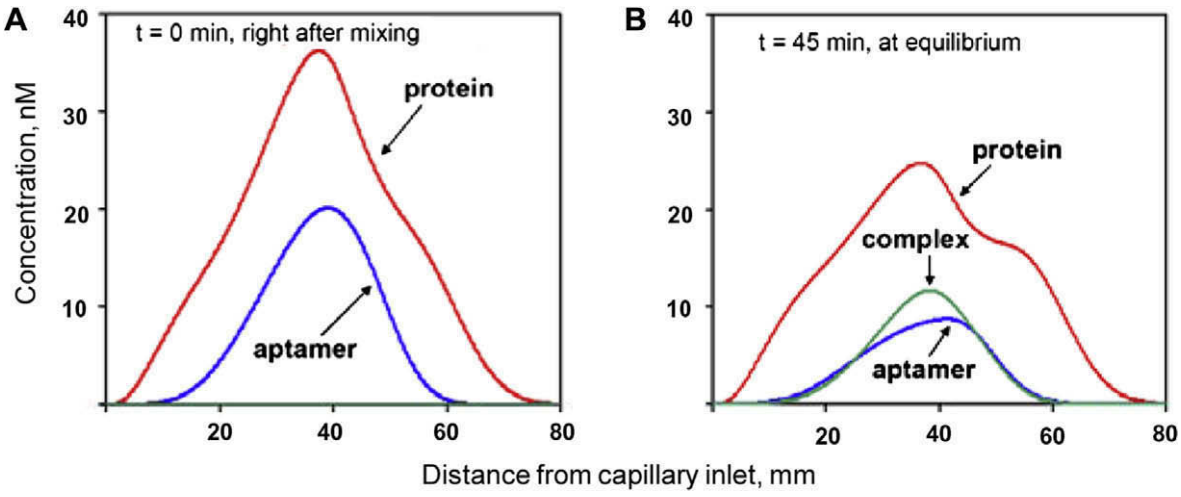

Figure 12. Numerically simulated concentration profiles of the protein, the aptamer and the protein-aptamer complex, right after mixing by TDLFP (**A**) and after equilibrium is reached (**B**). The mixing scenario was similar to that shown in Fig. 6**B** (Reprinted with permission from [1], © 2009 Elsevier).

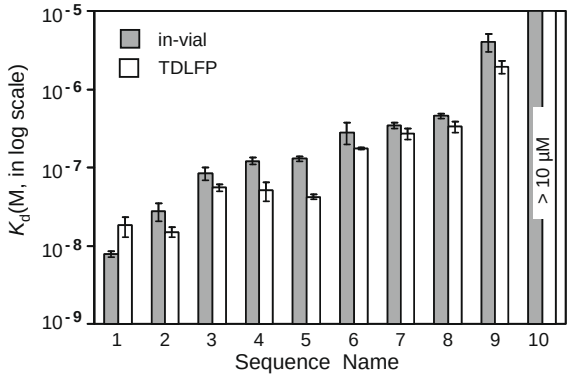

Figure 13. Ranking of DNA aptamers selected for MutS protein. K_d values for protein-aptamer interaction were measured with a kinetic capillary electrophoresis (KCE) method known as ''Non-Equilibrium Capillary Electrophoresis of Equilibrium Mixtures'' for mixing in a vial (grey bars) and TDLFP mixing in a capillary microreactor (white bars). The vertical axis is in a logarithmic scale (Reprinted with permission from [1], © 2009 Elsevier).

The combined simulation of two processes, TDLFP mixing and complex formation, was used in combination with the experimentally-determined amounts of the complex and unbound aptamer to calculate the equilibrium dissociation constant, K_d, of the complex (Fig 12).

By contrast to the β-galactosidase example, TDLFP simulation was performed numerically and included the effects of transverse diffusion during plug injection. Numerical simulation provided greater confidence in the accuracy of simulated concentration profiles.

To facilitate the determination of K_d, the binding reaction was modeled with varying K_d values, and simulated amounts of the complex and unbound aptamer were compared with the experimental values. The value of K_d, at which the simulated amounts of the complex and unbound aptamer were closest to the experimentally determined amounts, was considered to be correct. The accuracy of K_d determination was examined by measuring K_d with a conventional method, in which protein-aptamer binding was performed in a vial and the reaction mixture was sampled for KCE-based determination of K_d [1].

Fig. 13 compares K_d values measured in a TDLFP-facilitated capillary microanalysis (white bars) and the conventional CE analysis (grey) bars. There is a difference between the values obtained from the two methods. The origin of this difference most probably lies in a deviation of the real pressure dependence on time from a rectangular pressure pulse used in the simulations. However, the deviation is not significant and allows the use of the TDLFP-based integrated microanalysis for preliminary ranking of DNA aptamers and identifying suitable aptamers for more accurate measurements of K_d.

7.2.2. Mixing of four reactants. The advantage of mixing by TDLFP over mixing by electrophoresis or longitudinal diffusion is the ability of TDLFP to mix more than two separately-injected reactants. Mixing four reactants has recently done experimentally. It was in this study that the term IMReSQ was coined [21]. Enzymatic farnesylation of a pentapeptide, catalyzed by protein farnesyltransferase (FTase or E), was used in this work. The reaction involves two substrates, a fluorescently labeled CVGIA peptide (S1) as an acceptor of the farnesyl group and farnesyl pyrophosphate (FPP or S2) as a donor of the farnesyl group. The inhibition of this reaction was studied, so the reaction mixture had to include four components: the enzyme, two substrates and the FTase inhibitor (FTI or I).

First, TDLFP mixing of the four reaction components was studied using computer simulation by numerical solution. An algorithm for the optimization of the plug order in TDLFP mixing had not yet been developed, so, strictly speaking, the plug order could not be optimized. However, the concentration profiles of the mixed reaction components along the capillary for any given order of plugs could be simulated (Fig. 14A). Plug orders were tested using such a simulation, for which the orders seemed reasonable, based on the two simple criteria that the number of plugs had to be small, while the spatial overlap of the components after mixing had to be significant. The plug order chosen for the experimental mixing was S1, S2, E, I, and S1 again (see Fig. 14A). Plugs of an enzymatic buffer were injected before and after injecting the reaction components to:

(i) isolate the reaction mixture from the electrophoresis buffer that contained a surfactant; and,
(ii) improve the quality of mixing, respectively.

The simulated post-mixing concentration profiles of the four components did not overlap perfectly; however, they revealed a significant reaction zone in which all four components were present (Fig. 14A). There was also a reaction zone containing S1, S2, and E, but not I, suggesting that complete inhibition was not achievable with this mixing scenario.

In TDLFP, the required mixing time is defined by the time of transverse diffusion of the largest molecule (FTase, in this example). Computer simulation showed that, for the experimental conditions used, the time for sufficient mixing was less than 1 min. The reaction time was longer than the mixing time, which suggested that only a negligible amount of the product was formed during mixing.

It was also experimentally demonstrated that TDLFP mixed the four reactants and that product formation and inhibition were observed. The absence of either reactant meant that the concentration of the missing reactant in the injected plug was zero (a pure enzymatic buffer was injected instead of the corresponding reactant). In this

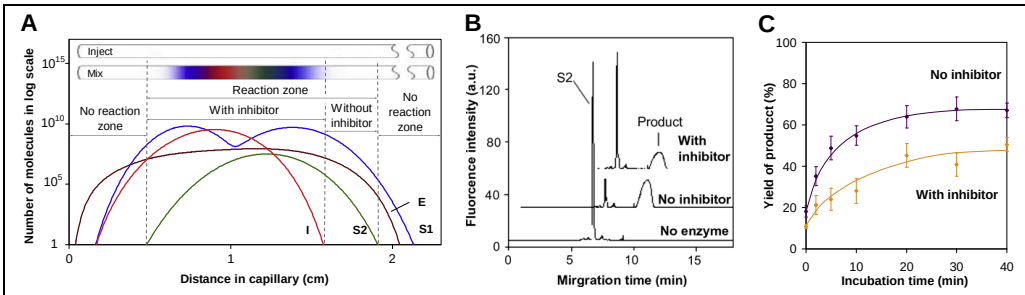

Figure 14. TDLFP-mediated capillary microanalysis (IMReSQ) for inhibition of enzymatic farnesylation of the fluorescently-labeled CVGIA peptide. **Panel A:** Simulated distribution of reaction components in the capillary after injection (**top**) and after mixing (**bottom**) for the following plug order: enzymatic buffer (white), FPP (S1, blue), fluorescent pentapeptide substrate (S2, green), FTase enzyme (E, brown), inhibitor (I, red), FPP again, and enzymatic buffer again. **Panel B:** Experimental results of IMReSQ analysis of FTase inhibition by a representative inhibitor (FTI-276) after 40-min incubation following injection and mixing of reaction components depicted in Panel A. The overlaid electropherograms are displaced along the time axis for clarity. The pre-injection concentrations were: 75 μM for S1, 0.2 μM for S2, 3 μM for E, and 50 μM for I. **Panel C:** Kinetics of product formation with and without inhibitor (50 μM FTI-276) (Reprinted with permission from [22], © 2008 American Chemical Society).

Table 2. IC_{50} and PIC_{50} for the inhibition of FTase-catalyzed farnesylation of CGVIA determined by traditional (in-vial reaction) and IMReSQ methods, respectively (Reprinted with permission from [22], ©2008 American Chemical Society)

Inhibitor	Traditional IC_{50} (μM)	IMReSQ PIC_{50} (μM)	PIC_{50}/IC_{50}
FTI-276	1.1 ± 0.3	11.2 ± 3.2	10.2 ± 2.9
FTI-277	2.1 ± 0.4	18.9 ± 3.8	9.0 ± 1.8
FTI-651	71 ± 17	800 ± 70	11.3 ± 2.7
FTI-656	61 ± 18	620 ± 90	10.2 ± 3.1

part of the study, the FTI-276 inhibitor, which had previously proved to inhibit mammalian FTase, was used to test the inhibition of FTase from *Entamoeba histolytica*, a parasite. When the concentration of E was zero, no P was formed and a single peak of S2 was detected (Fig. 14B, lower trace). In the presence of E but without I, S2 was converted into P and, accordingly, two peaks were observed after P was separated from the remaining S2 (Fig. 14B, middle trace). Finally, in the presence of I, the reaction rate was lower and the amount of P formed during the same incubation time was smaller. The peak of P was smaller, while the peak of the remaining S2 was bigger (Fig. 14B, upper trace) than those in the absence of I. When the incubation time varied, the reaction kinetics could be studied. In the absence and the presence of I, classical Michaelis-Menten kinetics was observed (Fig. 14C). Thus, all four components were mixed to the level at which the rate of P formation depended on [I].

The ability of the IMReSQ method to rank the potencies of inhibitors quantitatively was also tested. Conventionally, IC_{50} values (inhibitor concentrations that cause 50% reduction of the reaction rate) are used to rank inhibitors. IC_{50} depends on enzyme and substrate concentrations, so it is not applicable to IMReSQ, in which the solutions are not ideally mixed. To rank inhibitors by IMReSQ quantitatively, a new parameter, PIC_{50}, was suggested. PIC_{50} is a pre-injection inhibitor concentration that causes a 50% reduction in the reaction rate. Rankings of several potential inhibitors of FTase obtained by a ''traditional'' method, using IC_{50}, and by the IMReSQ method, using PIC_{50}, were compared. In the traditional method, mL volumes of S1, S2, I, and E were mixed in a vial and incubated to form P. A nL volume of the reaction mixture was injected into the capillary and P was separated from the remaining S2 and their amounts were quantitated. The PIC_{50}/IC_{50} ratio was identical within the error limits for all inhibitors (see Table 2).

The constant PIC_{50}/IC_{50} ratio suggested that IMReSQ can be used for quantitatively ranking the potencies of the inhibitors. Four inhibitors of mammalian FTase (FTI-276, FTI-277, FTI-651, and FTI-656) were found to be potent for FTase from *Entamoeba histolytica*. These compounds can therefore be used as templates for anti-parasite drug development. To conclude, TDLFP can facilitate the mixing of very complex reaction mixtures in the capillary, so it can facilitate IMReSQ integrated microanalyses for all types of enzyme.

7.2.3. cTDLFP-facilitated cell lysis for chemical cytometry. The generic capabilities of TDLFP contributed to further advances in chemical cytometry [21], which is a collective term applied to techniques that employ highly sensitive chemical-analysis instrumentation and methods to study the chemical contents of single cells quantitatively [22]. In chemical cytometry, the cell to be analyzed is first lysed to release its chemical contents from the cellular compartments and dissolve them in the surrounding buffer solution. The molecules of interest are then separated by CE or capillary chromatography and detected by laser-induced fluorescence (LIF), electrochemistry or MS.

CE-LIF is the most widely used combination of separation and detection in chemical cytometry, as CE can separate all kinds of biomolecule, and LIF can be used for the detection of single molecules.

TDLFP has proved to facilitate highly-efficient cell lysis inside the capillary for chemical cytometry [21]. A mild surfactant, Triton X-100, was used as lysing agent. It was either dissolved in the run buffer or its solution was introduced into the capillary by pressure as a short plug prior to cell injection. The cell was then injected by pressure within a plug of a physiological buffer. TDLFP was expected to mix the surfactant with the physiological buffer leading to surfactant contact with the cell and subsequent cell lysis. Cell lysis by a short plug of the surfactant was investigated to exclude the surfactant from the run buffer (as a surfactant in the run buffer can reduce the quality of CE separation).

To detect successful cell lysis, Madin-Darby canine kidney cells, expressing green fluorescent protein (GFP), were used in the experimental study. Fig. 15 shows electropherograms of intact and lysed cells corresponding to different scenarios of mixing. A very sharp spike-like peak with a migration time of 2–3 min was observed for intact GFP-expressing MDCK cell (Fig. 15A). When a run buffer was supplemented with a lysing agent, a wide peak corresponding to the GFP molecules dissolved in the run buffer was detected (Fig. 15B). Hence, the spike-like peak was employed as a criterion for a cell not being

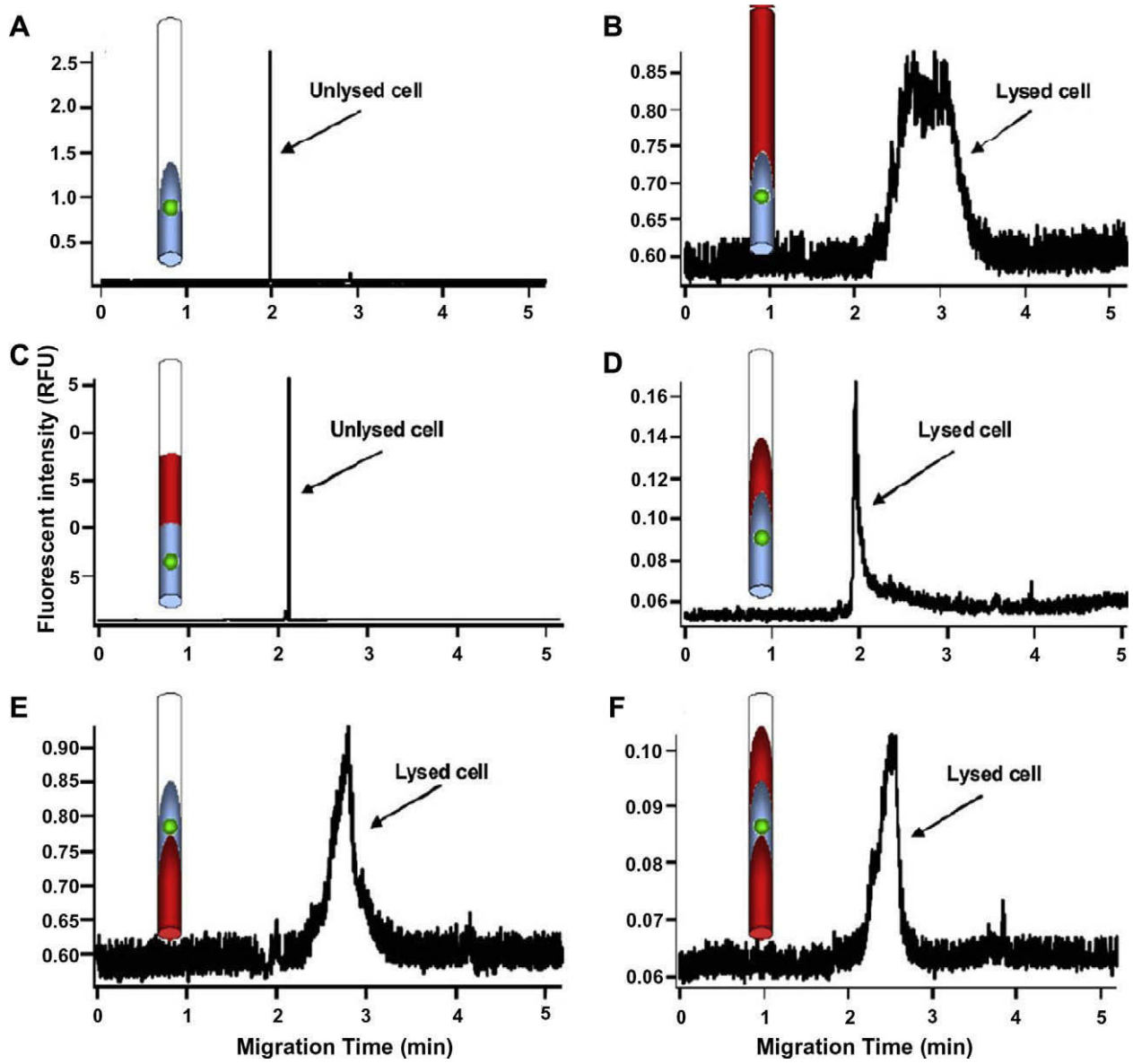

Figure 15. TDLFP-facilitated cell lysis in a capillary microreactor. Electropherograms of GFP-expressing cells under different scenarios of cell injection or lysis. Inserts show the corresponding scenarios of injection. The white color corresponds to the bare run buffer. The red color corresponds to the lysing agent (Triton X-100) dissolved in the run buffer. The blue color corresponds to the physiological buffer (phosphate buffered saline), in which the cells are suspended. The cell is shown as a green circle. **Panel A:** The inlet and the outlet reservoirs and the capillary contain the bare run buffer. A cell is injected by suction. **Panel B:** The inlet and the outlet reservoirs and the capillary contain the lysing agent. A cell is injected by suction. **Panel C:** The inlet and the outlet reservoirs and the capillary contain the bare run buffer. First, a plug of the lysing agent is injected into the capillary by an electric field. Second, a cell is injected by an electric field. **Panel D:** The inlet and the outlet reservoirs and the capillary contain the bare run buffer. First, a plug of the lysing agent is injected in the capillary by suction. Second, a cell is injected by suction. **Panel E:** The inlet and the outlet reservoirs and the capillary contain the bare run buffer. First, a cell is injected by suction. Second, a plug of the lysing agent is injected by suction. **Panel F:** The inlet and the outlet reservoirs and the capillary contain the bare run buffer. First, a plug of the lysing agent is injected by suction. Second, a cell is injected by suction. Third, another plug of the lysing agent is injected by suction (Reprinted with kind permission from [21], © 2006 Springer-Verlag).

lysed, while a wide peak of GFP was an indication of successful cell lysis inside the capillary. A wide peak of GFP combined with a sharp spike was interpreted as partial cell lysis, with a part of the cell remaining intact.

TDLFP-based cell lysis was performed using two-step and three-step injection, in which a plug of the lysing agent was introduced only before (two-step injection), only after (two-step injection), or both before and after (three-step injection) a plug of the physiological buffer with a cell. The observed results confirmed the hypothesis that TDLFP could facilitate the mixing of the surfactant with the physiological buffer and cause cell lysis.

TDLFP-based cell lysis was validated by comparing pressure-driven and EOF-driven injections. In general, plugs injected by EOF could be mixed only by longitudinal diffusion if not by electrophoresis. Longitudinal diffusion was expected to be much less efficient than TDLFP due to the high length/diameter ratios of the plugs. The experimental results were compared for two scenarios: first, when a single cell was injected by pressure for the TDLFP experiment; and, second, when a single cell was injected by electroosmosis for the longitudinal-diffusion experiment. When the surfactant and the cell were injected into the capillary by electroosmosis, the cells were left unlysed in 80% of experiments, and the cells were partially lysed in 20% of experiments. In the case of pressure-driven injection of the lysing agent and a cell, the cells were completely lysed in 80% of experiments and partially lysed in 20% of experiments. An even higher efficiency (100%) of TDLFP-driven cell lysis was achieved using the ''sandwich'' approach, in which plugs of the lysing agent were injected prior to and after the cell injection. These experiments confirmed that TDLFP facilitated efficient diffusion of the lysing agent towards the cell and promoted complete cell lysis. Lysis inside the capillary was methodologically and instrumentally simple. It also guaranteed that no losses of cellular components occurred. In addition to cell lysis, TDLFP could be used in chemical cytometry to mix cellular components with, e.g., labeling reactants, affinity probes and inhibitors.

8. Instrumentation for IMReSQ

There are currently about 20 commercially available CE instruments on the market [23–26], most of which offer options with electric-field-driven and pressure-driven injection. Many instruments also offer options with light-absorbance and fluorescence detection. Commercial instruments are typically not equipped with electrochemical or MS detectors, but such detectors can be custom-attached [27,28], so most commercial instruments suit the general requirements of IMReSQ.

However, there are limitations with respect to the use of commercial CE instruments for TDLFP-based IMReSQ. This mode of IMReSQ requires short pulses of high pressure with well-defined pressure profiles. Commercial CE instruments have relatively low limits of maximum pressure (typically 25 psi or less for injection) and relatively high limits of minimum time during which the pressure can be applied (usually 1 s or more). Moreover, commercial CE instruments do not include pressure gauges that would measure the exact time profiles of pressure, $\Delta p(t)$, used for injection. These instruments are also not optimized for fast change of vials required to decrease time between injections of parabolic plugs. The dead time is typically no shorter than 10 s. In some instruments, pressure-driven injection can be carried out only by suction, which limits Δp to less than 1 atm.

A separate issue is software. There is currently no commercial software to optimize injection/mixing scenarios and for the calculations that can be required in the downstream steps (Reaction, Separation, and Quantitation).

IMReSQ is an ideal approach for high-throughput screening (HTS). Accordingly, an instrument suitable for IMReSQ-based HTS should facilitate consequent analysis of multiple samples that can be achieved through using multiple capillaries or CE in multi-channel chips.

To conclude, the available CE commercial instruments provide a suitable base for IMReSQ-method development and use of IMReSQ in academic laboratories. For IMReSQ to be used in industrial application (e.g., HTS of drug candidates), a new generation of instrumentation is required to address the limitations identified above.

9. Conclusions and future outlook

We have demonstrated that IMReSQ satisfies the criteria of being both generic and quantitative in each of its steps. However, there is no ''one size fits all approach'' that can be adopted to optimize any particular reaction performed in capillary format. Each reaction will need to be considered according to its merits.

Whether pressure-driven or electroosmotic injection is employed will depend on whether an EOF can be produced in the capillary, the relative electrophoretic mobilities of the reactants and the number of reactants that need to be mixed. If pressure is used for injection, consideration should be given as to whether the goal is to achieve mixing of reactants or separation of the reaction mixture from a buffer component that could interfere with the reaction, when one type of pressure profile will not be suitable for each step of injection.

Mixing can be achieved by electrophoresis, longitudinal diffusion or TDLFP for volumes as small as one nL, greatly reducing the costs associated with expensive reagents. Of these mixing techniques, TDLFP has the advantages of being generic, robust and suitable for automation. In practice, electrophoretic mixing is suitable only for a maximum of two reactants with significantly different electrophoretic mobilities. Longitudinal diffusion is an option only for small molecules for which the coefficients of diffusion are relatively large; otherwise, the time taken is prohibitive. By contrast, TDLFP is highly efficient for mixing large molecules. Each of these mixing techniques can be described mathematically, allowing concentration profiles to be modeled accurately.

The best method of separation and quantitation will depend on the nature of reactants and products. Electrokinetic methods of separation are available for

charged and neutral species. Generally, universal methods of detection are less sensitive than selective detection methods employing fluorescence or amperometry.

Several examples of the generic and quantitative nature of IMReSQ have been demonstrated in the literature and have proved its worth in the fields of kinetics in microreactors, aptamer selection, chemical cytometry, and identification of inhibitors of interest to the pharmaceutical industry.

As far as the mathematical modeling of IMReSQ is concerned, there is still room for improvement in numerical methods of simulation. The current software makes no differentiation between sections of the capillary where no interactions occur and regions where interactions are taking place. By using a finer grid for only the regions where interactions are taking place, it will be possible to produce a better fit of the experimental data without compromising computer speed. However, the current software is suitable for most applications when Yo are very small (e.g., $Yo < 10^{-6}$), but there are cases when the solution becomes unstable. This problem can be overcome by using a finer grid so that more iteration occurs in the program, but this tends to compromise the speed of calculation. The mathematics to describe IMReSQ is now well understood, but the technology required for its wide-scale application is lagging behind.

For IMReSQ to become an attractive technique for parallel synthesis or for HTS applications in the pharmaceutical industry, instrumentation will need to be developed that can produce rapid pulses of high pressure precisely with well-defined pressure profiles in multiple-capillary chromatography and/or electrophoresis devices.

References

[1] D. Yunusov, M. So, S. Shayan, V. Okhonin, A. Petrov, S.N. Krylov, Anal. Chim. Acta 603 (2009) 102.
[2] S.N. Krylov, Electrophoresis 28 (2007) 69.
[3] S.N. Krylov, J. Biomol. Screen. 11 (2006) 115.
[4] P. Jandik, G.K. Bonn, Capillary Electrophoresis of Small Molecules and Ions, VCH, New York, USA, 1993.
[5] T. Kaneta, T. Ueda, K. Hata, T. Imaska, J. Chromatogr., A 1106 (2006) 52.
[6] J. Crank, The Mathematics of Diffusion, Oxford University Press, Oxford, UK, 1975.
[7] T.J. Kaiser, J.W. Thompson, J.S. Mellors, J.W. Jorgenson, Anal. Chem. 81 (2009) 2860.
[8] M.U. Musheev, S. Javaherian, V. Okhonin, S.N. Krylov, Anal. Chem. 80 (2008) 6752.
[9] G.I. Taylor, Proc. R. Soc. London, Ser. A 219 (1953) 186.
[10] V. Okhonin, E. Wong, S.N. Krylov, Anal. Chem. 80 (2008) 7482.
[11] S.M. Krylova, V. Okhonin, S.N. Krylov, J. Sep. Sci. 32 (2009) 742.
[12] P.S. Andersen, C. Jespersgaard, J. Vuust, M. Christiansen, L.A. Larsen, Hum. Mutat. 21 (2003) 116.
[13] E.M. Abad-Villar, J. Tanyanyiwa, M.T. Fernandez-Abedul, A. Costa-Garcıa, P.C. Hauser, Anal. Chem. 76 (2004) 1282.
[14] J.S. Kuo, C.L. Kuyper, P.B. Allen, G.S. Fiorini, D.T. Chiu, Electrophoresis 25 (2004) 3796.
[15] W.R. Vandaveer, S.A. Pasas, R.S. Martin, S.M. Lunte, Electrophoresis 23 (2002) 3667.
[16] R.M. Guijt, C.J. Evenhuis, M. Macka, P.R. Haddad, Electrophoresis 25 (2004) 4032.
[17] P. Kuban, P.C. Hauser, Electrophoresis 30 (2009) 176.
[18] J. Bao, F.E. Regnier, J. Chromatogr., A 608 (1992) 217.
[19] S. van Dyck, E. Kaale, S. Nováková, Z. Glatz, A. van Schepdael, Electrophoresis 24 (2003) 3868.
[20] V. Okhonin, X. Liu, S.N. Krylov, Anal. Chem. 77 (2005) 5925.
[21] M.V. Berezovski, T.W. Mak, S.N. Krylov, Anal. Bioanal. Chem. 387 (2007) 91.
[22] E. Wong, V. Okhonin, M.V. Berezovski, T. Nozaki, H. Waldmann, K. Alexandrov, S.N. Krylov, J. Am. Chem. Soc. 130 (2008) 11862.
[23] S.N. Krylov, D.A. Starke, E.A. Arriaga, Z. Zhang, N.W.C. Chan, M.M. Palcic, N.J. Dovichi, Anal. Chem. 72 (2000) 872.
[24] http://www.labx.com/v2/adsearch/results-new.cfm?PN=2&sw=Capillary%20Electrophoresis, 2009, p. labX.
[25] http://search.pro-talk.com/search?q=capillary+electrophoresis&spell=1&ie=&site=pro-talk&output=xml_no_dtd&client=pro-talk&access=p&lr=&proxystyle, p. Pro Talk website.
[26] http://test-equipment.globalspec.com/SpecSearch/Suppliers?Comp=2158, 2009, p. Global Spec Website.
[27] http://www.esainc.com/products/type/hplc_systems/detectors/fluorescencedetector, 2009, p. ESA Product information.
[28] http://www.unichrom.com/tracedec/tracedece.shtml, 2009, p. Innovative Sensor Technologies GmbH Product Information.